

PATTERNS OF DIVERSITY IN A GENETICAL MODEL OF BACTERIA-PHAGE COEVOLUTION

R. E. BEARDMORE, S. S. ARKIN, S. E. FORDE, AND I. GUDELJ

ABSTRACT. How does the supply of energy affect the diversity of an evolving microcosm? Two competing informal arguments might be proposed: an increase in energy boosts the proportion of energy-inefficient, fast-growing specialists thus reducing diversity. Or, a greater energy supply can support more niches that may, in turn, be exploited by a greater diversity of species.

We approach this question from the perspective of an evolutionary microcosm containing a co-evolving host and pathogen. The host is the bacterium *E.coli* B (strain EL606) and the pathogen is its bacteriophage, T3, supported by an environment whose limiting hydrocarbon resource is glucose. We perform a mathematical and experimental study of the biodiversity supported by this model system and propose that both hypothesised relationships are possible: diversity can be both negatively and positively correlated with energy supply. Moreover, the precise details of how this relationship is manifested in this model system depends crucially upon molecular and genetic details of the interaction between the host and its viral parasite.

1. INTRODUCTION: THE BEAGLE IN A BOTTLE

Natural ecosystems consist of many species interacting through diverse mechanisms, some of which may see one organism increase its reproductive ability to the detriment of another. This type of interaction occurs between predators and their prey and between pathogens and their hosts. *Antagonistic coevolution* is said to take place in a host-pathogen system whenever a defense strategy brought about in the host is countered by the evolution of a concomitant strategy in the pathogen, leading to an arms race often called the *Red Queen effect* [34].

Although antagonistic coevolution has been observed in natural ecosystems [38, 7], reproducing observations is difficult. Complex organisms often have small population sizes and long reproduction times, necessitating observations over many years and often leading to an incomplete fossil record.

Hoping to overcome such difficulties, evolutionary researchers have turned to the idea of *The Beagle in a Bottle* [4], laboratory microcosms of microbial populations that can be used to pinpoint the biological processes that generate and maintain diversity [8, 15, 5, 3]. Due to their large population sizes and short generations, *do novo* evolution can be observed within weeks over thousands of generations.

Key words and phrases. coevolutionary dynamics, ecological genetics, *E.coli* bacteria, T-series bacteriophage.

1.1. Productivity: diversity and energy. The purpose of this paper is to use a chemostat-based experimental microcosm to ask how changes in resource availability mediate the diversity observed in coevolving bacteria and bacteriophage populations. Moreover, resource availability in microbial experiments may be considered as an analogy of *productivity* in nature since it measures the energy available for conversion into biomass [5].

Discerning the relationship between productivity and diversity has been a major challenge in ecology and is thought to be a prerequisite to understanding patterns of diversity observed both within and across ecosystems [36]. Previous studies conducted on large data sets and spanning a range of geographical scales and species have revealed that this relationship can exhibit a positive correlation, a negative correlation, or be more complex still and several explanations for such variation have been proposed [18, 25, 13].

Previous laboratory studies of microbes competing for resources in spatially homogeneous environments have shown that diversity can increase monotonically as a function of productivity and that spatial structure may be needed in order to observe a unimodal relationship between diversity and productivity [17, 5]. In [13], the authors invoked heterogeneous resource supply as an explanation of such unimodal patterns. In contrast to these findings, a recent study of the bacterium *E. coli B* and its viral parasite, the T3-bacteriophage, undertaken by the present authors revealed that antagonistic coevolution can result in a unimodal or multimodal relationship between bacterial diversity and productivity [11]. The contribution of this paper is to provide details of the mathematical framework used in that experimental study.

In addition to their value as model systems for probing coevolutionary processes in general, bacteria-bacteriophage interactions are important in their own right. Bacteria constitute a vast proportion of the total DNA in the oceans [9] and they are major contributors both to primary production and to the cycling of nutrients through trophic levels [22]. As part of the microbiota, they also constitute about 99% of the total DNA in the human body where they process nutrients and protect the human host against diseases such as forms of *colitis* [23]. Bacteriophage not only regulate microbial population sizes but also their rate of adaptation and thus also impinge upon carbon and nutrient cycling and pathogenic diseases through the destruction of their hosts.

There is an increasing commercial interest in antibacterial treatments that use bacteriophages [32]. Although *bacteriophage therapy* has been an active field of research in the former Soviet republics, it received little attention in the West due to the advent of broad spectrum antibiotics [19]. However, the widespread use of antibiotics has resulted in the emergence of antibiotic-resistant bacterial strains and phage therapy is being taken seriously as a possible alternative for certain infections. The use of synthetic phage [20, 21] may, in time, make phage therapy a practicable alternative to antibiotics for such infections.

1.2. Description of the experimental model system. *Bacteriophage* are the viruses of eubacteria. The initial phase of infection of the bacterial host by the virus is *adsorption*, a process that takes place in at least two stages. First, specific proteins on the phage bind to receptor molecules such as the antigenic lipopolysaccharide (LPS) polymers (whose chemotypes are illustrated in Figure 1), lipoproteins or teichoic acids on the surface of the bacteria. This initial binding can be irreversible and electrostatic in nature [27] and is highly specific, meaning each species of phage can adsorb to only a small number of molecules on a limited number of bacterial species [29]. For example, the coliphage T4 is known to adsorb only to the LPS backbone on *E.coli*, a biopolymer used by the bacterium to maintain its structural integrity and impermeability [28], while the λ -phage is known to bind to the lamB maltoporin on *E.coli*.

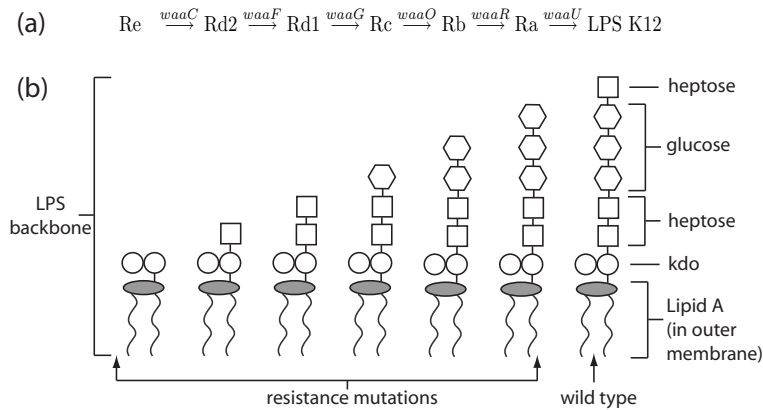


FIGURE 1. (a) Biosynthesis pathway for the lipopolysaccharide (LPS) biopolymer and (b) an illustration of the intermediate chemotypes that differ in their T3 resistance. In (a), names of the genes encoding the enzymes that catalyse the reaction steps are shown above the arrows and the designated names for the chemotypes are shown between the arrows [28].

Bacteria can gain resistance to phage through genetic mutations that lead to structural changes in the receptor molecules used by the phage during adsorption. As these molecules have various roles within the bacterial metabolism, mutations may affect the ability of the bacteria to function and replicate and so resistance mutations may, but not always, come with a *fitness cost* to bacteria.

The initial binding may be followed by a secondary, irreversible binding between the bacterium and specific proteins on the phage within the capsids or tail fibres, depending on the specific phage [29]. Adsorption is then followed by injection of the phage genome into the bacterial cytoplasm directly through the membrane or through specific outer-membrane proteins (OMPs), after which the phage life cycle can follow one of at least two paths depending on the type of phage involved.

If the phage is of the *lytic* or virulent kind, it uses the bacterial metabolism to make copies of the viral genome and the proteins which constitute its structural components. Subsequently, these molecules self-assemble into complete phage particles and exit the cell with the help of enzymes that degrade, or lyse, the bacterial membrane. The bacterial cell is destroyed in this process and the number of phage particles or *virions* produced per bacterial death is termed the *burst size*.

If the phage is of the *lysogenic* or temperate kind, its genome can be incorporated into the bacterial genome and it can remain there as a *prophage*, replicating with the bacteria until such time as the environmental conditions favour the return of the prophage to the lytic state. Other phage types exist too, such as the filamentous M13 phage synthesised in [21] that can replicate without lysing the bacterial cell.

The fitness cost of resistance to phage attack is usually expressed as a reduction in bacterial growth rate [3]. However, it is essential to note that because of the metabolic and physiological function of the phage target molecules, the precise nature of any fitness cost may depend crucially on the resources present in the environment. Thus, in order to ensure that mutations *necessarily* come with an associated fitness cost to the bacteria, we study a microcosm containing *E.coli B* with T3 phage under *glucose* limitation. The evolutionary dichotomy for the bacteria is the following: a genetic mutation that truncates the LPS polymer will impair the ability of the cell to metabolise glucose, however, it will also reduce the likelihood of being lysed by the phage. So, which evolutionary outcome will result from this interaction?

1.3. Notation. We make extensive use of the n -dimensional vectors $\mathbf{1} = (1, \dots, 1)$ and $\mathbf{0} = (0, \dots, 0)$ throughout. Given $\mathbf{u} = (u_1, \dots, u_n), \mathbf{v} = (v_1, \dots, v_n) \in \mathbb{R}^n$, the inequality $\mathbf{u} \geq \mathbf{v}$ will be used to mean $u_j \geq v_j$ for all j , $\mathbf{u} > \mathbf{v}$ will be used if $\mathbf{u} \geq \mathbf{v}$ but $u_j > v_j$ for some j , while $\mathbf{u} \gg \mathbf{v}$ will be used when $u_j > v_j$ for all j . Their inner product will be represented by (\mathbf{u}, \mathbf{v}) and therefore $(\mathbf{1}, \mathbf{v}) = \|\mathbf{v}\|_1 = \sum_{i=1}^n v_i$ for $\mathbf{v} \geq \mathbf{0}$. Pointwise operations of multiplication and division will be written without reference to any binary operator, so $\mathbf{u}\mathbf{v} = (u_1v_1, \dots, u_nv_n)$ and $\mathbf{u}/\mathbf{v} = (u_1/v_1, \dots, u_n/v_n)$.

For a linear map or matrix $\mathbf{A} : \mathbb{R}^n \rightarrow \mathbb{R}^n$, $\rho(\mathbf{A})$ will denote its spectral radius, $N(\mathbf{A})$ its null-space and $R(\mathbf{A})$ its range. Given a vector $\mathbf{u} \in \mathbb{R}^n$, $\text{diag}(\mathbf{u})$ will refer to the diagonal $n \times n$ matrix with entries: $(\text{diag}(\mathbf{u}))_{ii} = u_i$ for $i = 1, \dots, n$.

The term *diversity measure* will refer to any scale-invariant, permutation-invariant and positive functional $H : \mathbb{R}^n \rightarrow \mathbb{R}$ that is continuous away from zero, maximised at the ‘uniform state’ and minimised at the *competitive exclusion* state:

$$H(1, 1, \dots, 1) = \sup_{\mathbf{v} > \mathbf{0}, \mathbf{v} \in \mathbb{R}^n} H(\mathbf{v}) \quad \text{and} \quad H(1, 0, \dots, 0) = \inf_{\mathbf{v} > \mathbf{0}, \mathbf{v} \in \mathbb{R}^n} H(\mathbf{v}).$$

We therefore also require H to satisfy $H(s\mathbf{v}) = H(\mathbf{v})$ and $H(P\mathbf{v}) = H(\mathbf{v})$ for all $\mathbf{v} \in \mathbb{R}^n$ with $\mathbf{v} > \mathbf{0}$, for all permutations P and all scalars $s > 0$.

Common diversity measures are entropy, or the so-called *Shannon-Wiener diversity index*, $H_{sw}(\mathbf{v}) := -\sum_{i=1}^n \ln(v_i/(\mathbf{1}, \mathbf{v})) v_i/(\mathbf{1}, \mathbf{v})$ and *Simpson's index*

$$H_s(\mathbf{v}) := 1 - (\mathbf{v}, \mathbf{v})/(\mathbf{1}, \mathbf{v})^2.$$

2. A MATHEMATICAL MODEL

We shall define a mathematical model of *E.coli*-T3 phage coevolution in the chemostat based on the following assumptions:

- (A1.) The chemostat has a constant *dilution rate*.
- (A2.) Bacterial cells require many resources but only one hydrocarbon source is limiting and it is fed into the chemostat at the dilution rate. Furthermore, this *limiting nutrient* has no inhibitory effects on the bacteria at high concentrations, thereby the bacterial growth rate increases monotonically with increasing resource concentration.
- (A3.) Each bacterial cell belongs to one of a fixed number of genetically distinct *types*. Types differ in the structure of their outer membrane proteins and polysaccharides involved in phage and resource adsorption, they therefore have different growth rates and different abilities to resist phage infection.
- (A4.) Each phage belongs to one of a fixed number of genetically distinct types. Phage types differ in the structure of their tail proteins and thus in the range of bacterial types they can infect, the rate at which they adsorb to different bacterial types and in their burst sizes.
- (A5.) The chemostat is well mixed, ensuring that the concentration of the limiting nutrient is uniform in space and the rate of encounter between a phage particle and a bacterial cell follows a mass-action law.
- (A6.) Phage types are obligately lytic and all successful adsorption events lead to bacterial death.
- (A7.) After binary fission and virion assembly, respectively, there is a small but non-zero probability that offspring bacteria and phage will be of a different type to their parent.

Assumption A5 was verified empirically for T4 phage, up to a concentration of 5×10^8 bacterial cells per millilitre [12] some time ago, which justifies its use here. One can employ further assumptions to simplify or widen the particular class of models one defines. For example, there is a hierarchy of possibilities relating to A6 and A7. One might, for example, ask how important the *latent period* is in the phage replication process. This is the time taken to synthesise and assemble phage proteins into a complete virion and its inclusion may require a time delay, a complicating factor we chose not to include in our models below.

Assumption A7 states that genetic mutations occur during reproduction. However, since phage reproduction occurs within a bacterial cell, one might also ask how the architecture of the host influences phage mutations. In this paper we will make the

simplifying assumption that mutations in the phage genome are independent of the type of the bacterial cell in which phage replication takes place. Moreover, horizontal gene transfer and the mechanisms that support it will be neglected entirely. We also assume for simplicity that assembled virions are stable in the liquid medium of the culture vessel and do not decay, but this can be weakened in our analysis below.

2.1. Genetics: mutational assumptions. Suppose for simplicity that there are n possible bacterial types. In accordance with A7, when a bacterial cell of type $j \in \{1, 2, \dots, n\}$ divides there is a non-zero probability that one of its two daughter cells will be of type $i \in \{1, 2, \dots, n\}$ and we denote this probability by m_{ij} , so that

$$m_{ij} = P(\text{daughter bacterial type} = i | \text{parent bacterial type} = j \cap \text{a mutation occurs}).$$

It follows that $m_{ii} = 0$ and that $0 \leq m_{ij} \leq 1$ with $\sum_{i=1}^n m_{ij} = 1$ for all j .

Define the diagonal matrix $\mathcal{E} = \text{diag}(\epsilon_1, \dots, \epsilon_n)$ where ϵ_j is the per unit time, per cell mutation rate of bacterial type j and set $M = (m_{ij})$. We will call $\mathcal{M} := I + (M - I)\mathcal{E}$ a *mutation operator* and M a *mutation process*. If $\mathcal{E} = \epsilon I$, so that the mutation rate is the same for all types, then we will write

$$\mathcal{M}_\epsilon = I + \epsilon(M - I)$$

to emphasise the dependence on ϵ .

As $\mathbf{1}^T M = \mathbf{1}^T$ and so $\mathbf{1}^T \mathcal{M}_\epsilon = \mathbf{1}^T$ for all $\epsilon \in (0, 1)$, if M is an irreducible matrix then there is a unit 1-norm vector $\boldsymbol{\nu} \geq 0$ independent of ϵ such that $M\boldsymbol{\nu} = \boldsymbol{\nu}$ and therefore

$$\mathcal{M}_\epsilon \boldsymbol{\nu} = \boldsymbol{\nu}, \quad (\mathbf{1}, \boldsymbol{\nu}) = 1,$$

this follows from the Perron-Frobenius theorem. We shall further assume throughout that $\mathcal{M} - I$ is strictly negative definite with respect to its invariant space $V := \langle \mathbf{1} \rangle^\perp$ in the sense that

$$(1) \quad \rho_0 := - \sup_{\mathbf{v} \in V, \|\mathbf{v}\|_2=1} ((\mathcal{M} - I)\mathbf{v}, \mathbf{v}) > 0.$$

2.2. The coevolutionary model. Consider the following system of differential equations,

$$(2a) \quad \frac{d\mathbf{b}}{dt} = \mathcal{M}(\mathbf{B}(S)\mathbf{b}) - d\mathbf{b} - (\Phi\mathbf{p})\mathbf{b},$$

$$(2b) \quad \frac{d\mathbf{p}}{dt} = \mathcal{M}_p(\boldsymbol{\beta}(\Phi^T\mathbf{b})\mathbf{p}) - d\mathbf{p},$$

$$(2c) \quad \frac{dS}{dt} = d(S_0 - S) - (\mathbf{U}(S), \mathbf{b}).$$

Here $\mathbf{b} = (b_1(t), \dots, b_n(t))^T$ and $\mathbf{p} = (p_1(t), \dots, p_n(t))^T$ are non-negative vectors containing the density of bacterial cells and phage virions per millilitre, respectively, and $\boldsymbol{\beta} = (\beta_1, \dots, \beta_n)^T$ is the positive vector of phage burst sizes. Furthermore, \mathcal{M}_p denotes an irreducible *phage mutation operator* constructed analogously to the bacterial mutation operator \mathcal{M} .

To each bacterial type i we assign its growth rate $B_i(S)$, a function of the nutrient concentration S and of the inherited trait through the index i . By assumption A3 we impose the following conditions on $B_i(S)$ for $i \in \{1, \dots, n\}$:

- (B1.) $B_i(S_1) < B_i(S_2)$ when $0 \leq S_1 < S_2$,
- (B2.) $B_i(S) = 0$ if and only if $S = 0$ and
- (B3.) $\lim_{S \rightarrow \infty} B_i(S) = \overline{B}_i$ for a positive, finite constant \overline{B}_i .

For convenience later, let us define the vector of maximal growth rates $\overline{\mathbf{B}} := (\overline{B}_1, \overline{B}_2, \dots, \overline{B}_n)$.

Remark 1. *We will make extensive use of the bounded, monotonic increasing Monod function*

$$(3) \quad \Lambda(S) := \frac{S}{K + S}$$

throughout the paper.

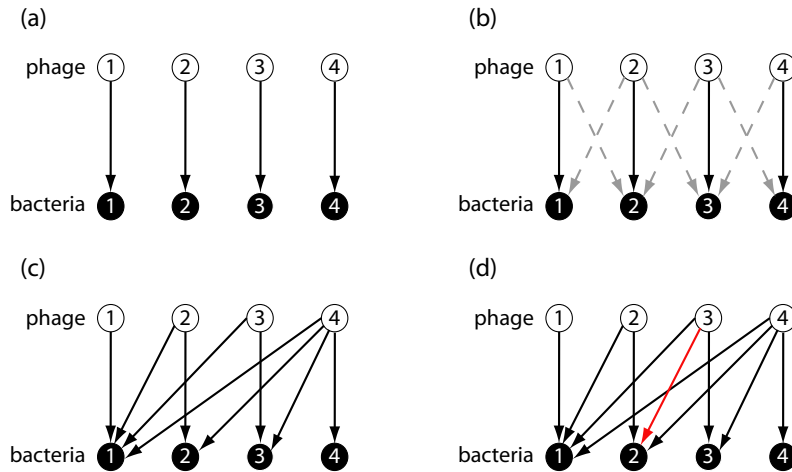


FIGURE 2. Graphs illustrating bacteria-phage cross-resistance: (a) matching alleles, (b) imperfect lock-and-key, (c) gene-for-gene and (d) modified gene-for-gene adsorption mechanisms. The nodes represent bacteria and phage types while an arrow from a phage type to a bacterial type indicates that the phage type can adsorb to that bacterial type. Dashed arrows in (b) represent small adsorption rates. Note that (c) does not have the red arrow highlighted in (d), this difference ensures that (d) is not a strict gene-for-gene model.

2.3. The genetics of adsorption: the matrix Φ . In studies of host-pathogen interactions it has been proposed that infection mechanisms are to be found on a

continuum that ranges from the *gene-for-gene* to *matching alleles* mechanisms [1]. The former assumes that each phage type has a bacterial type to which it preferentially binds, as depicted in Figure 2(a/b), the latter is less straightforward and is depicted in Figure 2(c).

The logic of the gene-for-gene interaction is based on the following rationale. Suppose that the bacterial genome carries one of two alleles at two different loci and denote these alleles by S and R , which stand for *susceptible* and *resistant* to infection, respectively. Suppose that the phage genome also has two loci, each of which can carry the alleles V and A that represent *virulent* and *avirulent* infection strategies. This system contains a total of four bacterial types and four phage types, whence their adsorption matrix Φ is a 4×4 matrix.

Now define an ordering of these alleles in the sense that

$$V \overset{\text{infects}}{>} R \overset{\text{resists}}{>} A \overset{\text{infects}}{>} S,$$

and assume that each phage type is defined by the pair of alleles (P, p) . Consider a rule which states that a phage infects a bacterium, itself defined by the ordered pair (B, b) , if and only if both

$$(P > B) \text{ and } (p > b),$$

where $P, p \in \{V, A\}$ and $B, b \in \{S, R\}$.

So, for example, both phage types (V, A) and (V, V) can infect bacterial types (R, S) and (S, S) . One can describe the logic of this particular infection process succinctly with the adsorption matrix

$$\Phi_{G4G} = \theta \cdot \begin{bmatrix} 1 & 1 & 1 & 1 \\ 0 & 1 & 0 & 1 \\ 0 & 0 & 1 & 1 \\ 0 & 0 & 0 & 1 \end{bmatrix}$$

and this is called a *gene-for-gene interaction*. The constant θ in Φ_{G4G} is a baseline value for the wild-type bacteria-to-phage adsorption rates [12].

Suppose that the wider the range of bacterial types a phage type can infect, the lower its adsorption rate must be to each of the bacterial types. Such a trade-off that describe the costs of virulence and resistance can easily be incorporated into the adsorption matrix, Φ , and [1] includes structures to account for this. For example, the adsorption matrix given by

$$\Phi_{g4g} = \theta \cdot \begin{bmatrix} 1 & \frac{1}{2} & \frac{1}{2} & \frac{1}{4} \\ 0 & \frac{1}{2} & 0 & \frac{1}{4} \\ 0 & 0 & \frac{1}{2} & \frac{1}{4} \\ 0 & 0 & 0 & \frac{1}{4} \end{bmatrix}$$

can be obtained by setting $a = 1$ and $k = \frac{1}{2}$ in Table 1 of [1] and it incorporates the aforementioned trade-off.

The adsorption mechanisms between phage and bacterium depend on a variety of molecular interactions and are not known in any generality. The *matching alleles* mechanism is believed to arise when adsorption has a high degree of specificity [37]. For example, the interaction between the λ -phage and the lamB maltoporin on *E. coli* has been hypothesised to be an imperfect lock-and-key mechanism that one can view as a form of approximate matching alleles interaction [37]. The matching alleles mechanism is represented by a diagonal matrix and if, in addition, the adsorption rates between all bacteria and phage types are equal, in this case one can write

$$\Phi_{MA} = \theta \cdot I_{4 \times 4},$$

where $I_{4 \times 4}$ is an identity matrix.

3. A CASE STUDY: AN *E. coli*-T3 COEVOLUTIONARY EXPERIMENT

We performed a series of coevolutionary experiments to probe how changes in resource availability would mediate the observed diversity of bacteria and phage. The experiments were conducted in chemostats with a constant dilution rate using the host bacterium *E. coli* B(EL606) with *glucose* as the limiting resource and using T3-phage. We now summarise the outcome of that experiment and its main results, referring to [11] for complete details of the experimental methodologies.

Samples were taken from the chemostats at three and nineteen days, the latter at about 150 bacterial generations. Those samples were screened for bacterial strains resistant to the wild-type phage and for the existence of genetic mutations that are known to result in alterations in the LPS antigen and membrane-bound ompF and ompA proteins. This was done using a variety of reference phage that are known to target these molecules as binding sites.

The resulting data was used to determine the frequency of OMP and LPS mutations found in bacteria isolated from the chemostats at the end of the 19-day period. Thus a measure of system ‘diversity’ could be calculated by determining the relative densities of bacterial cells that possessed structural changes in LPS, outer-membrane proteins or both, giving a total of four bacterial phenotypes.

3.1. Experimental observations: summary. At very low glucose concentrations, specifically when $S_0 \ll 10\mu\text{g/ml}$, the phage population cannot be supported and so the wild-type *E. coli* cannot coevolve with T3. As a result, no experiments were conducted at such low concentrations.

At higher glucose supply concentrations, $S_0 \geq 10\mu\text{g/ml}$, Figure 3(left) illustrates the main experimental outcome in terms of the mean observed frequencies (taken over three replicates) of each bacterial mutant at ‘low’ and ‘high’ resource supply levels. We highlight the following features of the data:

- At $S_0 = 10\mu\text{g/ml}$, Figure 3(left/LOW) shows that three bacterial strains are present in this environment and the dominant strain is one with alterations in both its LPS and OMP structure.

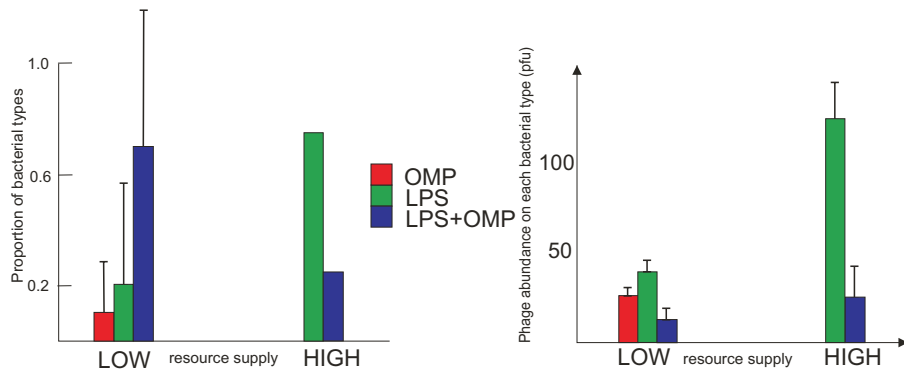


FIGURE 3. Experimentally-observed mutants at day nineteen: frequency of different bacteria (left) and the abundance of phage on these strains (right) at two different glucose supply values. (LOW means $10\mu\text{g}/\text{ml}$ and HIGH means $1000\mu\text{g}/\text{ml}$. A bar represents one standard error. The wild-type bacteria were not detectable and are therefore absent from the left-hand figure.)

- At $S_0 = 1000\mu\text{g}/\text{ml}$, Figure 3(left/HIGH) shows that bacterial diversity (measured by *Simpson's index*) is lower than microcosms for which $S_0 = 10\mu\text{g}/\text{ml}$ as the device no longer supports OMP-only mutants. Here, the dominant bacterial strain has the LPS-only mutation and the bacterial type with both LPS and OMP alterations is subdominant.

Observe that the wild-type *E.coli* strain does not appear at all in Figure 3(left) as it could not be isolated from the microcosm at measurable densities. Figure 3(right) shows the phage abundance in terms of *plaque forming units* obtained using phage isolated from the chemostat at day nineteen when tested on each of the four different bacterial types. This diagram does not, however, illustrate phage diversity. The latter could not be measured using this data as host-range phage mutants could not be isolated.

We summarise Figure 3 with the following coarse statement: *higher concentrations of abiotic resource supply support lower bacterial diversity.*

3.2. A model specific to *E.coli* and T3. We will assume for simplicity that just three mutant bacteria and phage are possible in (2), in addition to the wild-type, and so we set

$$\mathbf{b} = (b_0, b_1, b_2, b_3) \quad \text{and} \quad \mathbf{p} = (p_0, p_1, p_2, p_3);$$

the subscript zero in either of the two vectors \mathbf{b} and \mathbf{p} denotes the wild-type.

The phage mutation process \mathcal{M}_p in (2) is based on the Jukes-Cantor 69 substitution model (JC69) [16, 10] and, in the absence of clear evidence supporting the use of other mutational models, we use it to represent changes in the phage genotype that regulate the expression of tail-fibre proteins. We will assume for simplicity that a single locus within the phage genome encodes one of four alleles corresponding to four different

tail-fibre configurations. We further assume that mutations change the allele at this locus to any of the four allowed with equal probability. So, we define

$$M_p = \frac{1}{3} \begin{bmatrix} 0 & 1 & 1 & 1 \\ 1 & 0 & 1 & 1 \\ 1 & 1 & 0 & 1 \\ 1 & 1 & 1 & 0 \end{bmatrix} \quad \text{and then set} \quad \mathcal{M}_p := I + \epsilon(M_p - I).$$

We will use a standard point mutation structure on two independent loci for \mathcal{M} in (2). One locus codes for the LPS structure, the other codes for the OMP structure. For these two loci, OMP and LPS that we will write as O and L for brevity, we assume that O and L take values in $\{0, 1\}$, where a ‘1’ in either locus denotes a mutation with respect to the wild-type. Thus, OL -pairs take values in the set $\mathcal{G} = \{00, 01, 10, 11\}$ and we now require a mutation process on \mathcal{G} .

The first part of this process, M_1 describes the change in genotype that occurs when only one mutation occurs at some locus, the second, M_2 , describes the change in genotype that occurs when two mutations occur simultaneously at different loci. Thus, we set

$$M_1 = \begin{bmatrix} 0 & 1 & 1 & 0 \\ 1 & 0 & 0 & 1 \\ 1 & 0 & 0 & 1 \\ 0 & 1 & 1 & 0 \end{bmatrix} \quad \text{and} \quad M_2 = \begin{bmatrix} 0 & 0 & 0 & 1 \\ 0 & 0 & 1 & 0 \\ 0 & 1 & 0 & 0 \\ 1 & 0 & 0 & 0 \end{bmatrix}$$

and define

$$\mathcal{M} := I + \epsilon(M_1 - 2I) + \epsilon^2(M_2 - I).$$

Both \mathcal{M}_p and \mathcal{M} are symmetric stochastic matrices and so their invariant density is given by $\nu = \frac{1}{4}(1, 1, 1, 1)^T$.

It is known that genes controlling LPS synthesis and outer-membrane protein assembly interact pleiotropically because of a biophysical interaction: some OMPs do not trimerise to form porins unless LPS has a certain minimal structure [30]. It is also known that mutations in genes associated with OMP synthesis can alter the nature of the LPS expressed [35]. Although it is impossible to capture such detail in a model like (2), in order to include a sense of these very complex interactions, we introduce a phenotype $\ell(L, O)$ to describe the ordering of susceptibilities of different bacterial types to each T3 type.

As there is a correlation between the length of the LPS backbone expressed by a bacterial cell and the susceptibility of that cell to T3 attack, the relative rank of this susceptibility will be determined by the value of the phenotype

$$\ell(L, O) := 4 - (2 \cdot L + O).$$

This provides four bacterial phenotypes: the wild-type b_0 with $(L, O) = (0, 0)$ and so $\ell = 4$ has the longest LPS backbone and is susceptible to the highest number of T3 types. Then there is b_1 , the OMP-only mutant with $(L, O) = (0, 1)$ and $\ell = 3$, there

is an LPS mutant type b_2 with $(L, O) = (1, 0)$ and $\ell = 2$. Finally we have b_3 , the OMP+LPS mutant type with $(L, O) = (1, 1)$ and $\ell = 1$, this has the shortest LPS backbone and so is resistant to largest number of T3 types among all the bacterial mutants.

3.3. T3 - *E.coli* B adsorption genetics. We implemented a resistance-growth rate trade-off for this microcosm whereby an increase in the range of resistance to phage through changes in LPS structure leads to a decrease in growth rate due to a loss of affinity for glucose [11, 2, 33, 26]. As a result, wild-type *E.coli* B is the least phage-resistant bacterial type but it has the highest uptake rate of glucose, while b_3 is the most resistant type but it has the lowest uptake rate of glucose.

We also assume an infectivity-growth rate trade-off in the phage whereby an increase in the number of hosts a phage can infect comes at a reproductive cost [6, 24]. Therefore wild-type phage has the smallest host range but the highest adsorption rate and burst size, whereas p_3 has the largest host range but the lowest adsorption rate to each bacterial type and the lowest burst size.

In order to mimic the ‘cooperation process’ between T3 tail fibres and the LPS molecule of *E.coli* B alluded to in [29], we assume that a mutation at either locus, L or O , reducing LPS length also reduces the binding affinity of the cell for *every* phage. Moreover, we assume that there is a certain LPS truncation beyond which no phage mutant can adsorb to the cell, apart from a highly virulent phage, p_4 .

This, as with gene-for-gene systems, yields a triangular structure for the adsorption matrix Φ . We included two *infectivity parameters* μ and ν in the definition of the experiment-specific Φ , each parameter describes the rate of decrease of adsorption rate with each bacterial mutation and the analogous rate of increase with each phage infection. These changes are assumed to follow a power-law distribution with respect to LPS length, resulting in the matrix

$$(4) \quad \Phi_{mG4G}(\nu, \mu) = \theta \begin{bmatrix} 1 & \mu & \mu^2 & \mu^3 \\ 0 & \nu\mu & \nu\mu^2 & \nu\mu^3 \\ 0 & 0 & \nu^2\mu^2 & \nu^2\mu^3 \\ 0 & 0 & 0 & \nu^3\mu^3 \end{bmatrix}.$$

Hence if $\nu \in (0, 1)$, $\Phi_{mG4G}(\nu, \mu)$ encodes a resistance-growth rate trade-off of the bacteria, while because of the ordering of the entries in the vector β , $\mu \in (0, 1)$ corresponds to an infectivity-burst size trade-off in phage; note that the adsorption rate of wild-type bacteria to wild-type phage in (4) is given by $\theta := 2 \cdot 10^{-8}$ ml/cell/h. The remaining parameters, ν and μ , are as yet unknown and are to be determined from a data-fitting procedure.

We say that the matrix Φ_{mG4G} represents a *modified* gene-for-gene interaction matrix because it has a sparsity pattern that differs from Φ_{G4G} and Φ_{g4g} in only one entry; this is the bold highlighted entry in the matrix (4), an entry that is zero in the

TABLE 1. The parameters used in the mathematical model (2) that produced the comparison with empirical data shown in Figure 3; parameters were determined either from the literature or further experiments (as described in [11]).

<i>parameter</i>	<i>description</i>	<i>value</i>
$\boldsymbol{\mu}_{\max}$	maximal growth rates	$(1.18, 1.009, 0.89, 0.66) h^{-1}$
C	growth yield	$4.35 \times 10^4 \text{ cells}/\mu\text{g}$
K	bacterial half-saturation constant	$0.06 \mu\text{g}/\text{ml}$
β	burst sizes	$(306, 153, 99, 72) \text{ virions}$
d	dilution rate	$0.2 h^{-1}$
ϵ	mutation rate	$10^{-4} \text{ cell}^{-1} \text{ division}^{-1}$
θ	wt-to-wt adsorption rate	$2 \cdot 10^{-8} \text{ ml}/\text{cell}/\text{h}$
ν, μ	fitted adsorption parameters	$\nu = 0.636, \mu = 0.94$

gene-for-gene interactions of [1]. Strictly speaking, therefore, Φ_{mG4G} is not a gene-for-gene adsorption matrix even though it describes an expanding host range of the evolving phage.

3.4. Comparison of model with experiment. We now compare the relative rank abundances obtained using the mathematical model (2) to those obtained empirically and shown in Figure 3. For this purpose, equation (2) is deployed with the model parameters that define the four-phenotype model detailed in this section and defined in Table 1.

So, the glucose uptake rates of bacterial types are given by the vector $\mathbf{U}(S) := \mathbf{V}_{\max} \cdot \Lambda(S)$, where \mathbf{V}_{\max} is the maximal resource uptake rate and is defined by $\boldsymbol{\mu}_{\max}/C$. The Monod function $\Lambda(S)$ was defined in (3) and its form ensures that all bacterial types have the same glucose half-saturation constant K . We assumed that all bacterial cells have the same growth yield C and so bacterial growth rates are provided by the vector $\mathbf{B}(S) = \boldsymbol{\mu}_{\max} \cdot \Lambda(S)$. Finally, we implemented the *modified gene-for-gene* matrix $\Phi_{mGFG}(\nu, \mu)$ within the model.

The mutation rate parameter ϵ for this modelling framework cannot be easily related to per-genome or per-nucleotide mutation rates. For this model, it was simply reduced to the smallest value for which equilibrium solutions of (2) could be reliably computed for all necessary values of S_0 using a continuation-Newton algorithm.

Other parameters were taken either from previous literature or found using calibration experiments detailed (see [11] for details). The infectivity parameters ν and μ were obtained from a fitting procedure whereby the relative abundances at equilibrium of each mutant were computed using (2) at $S_0 = 10 \mu\text{g}/\text{ml}$ and $S_0 = 1000 \mu\text{g}/\text{ml}$. The infinity-norm distance between the computed relative rank abundances from the model was then minimised with respect to the empirical rank abundances, thus providing the values of ν and μ in Table 1.

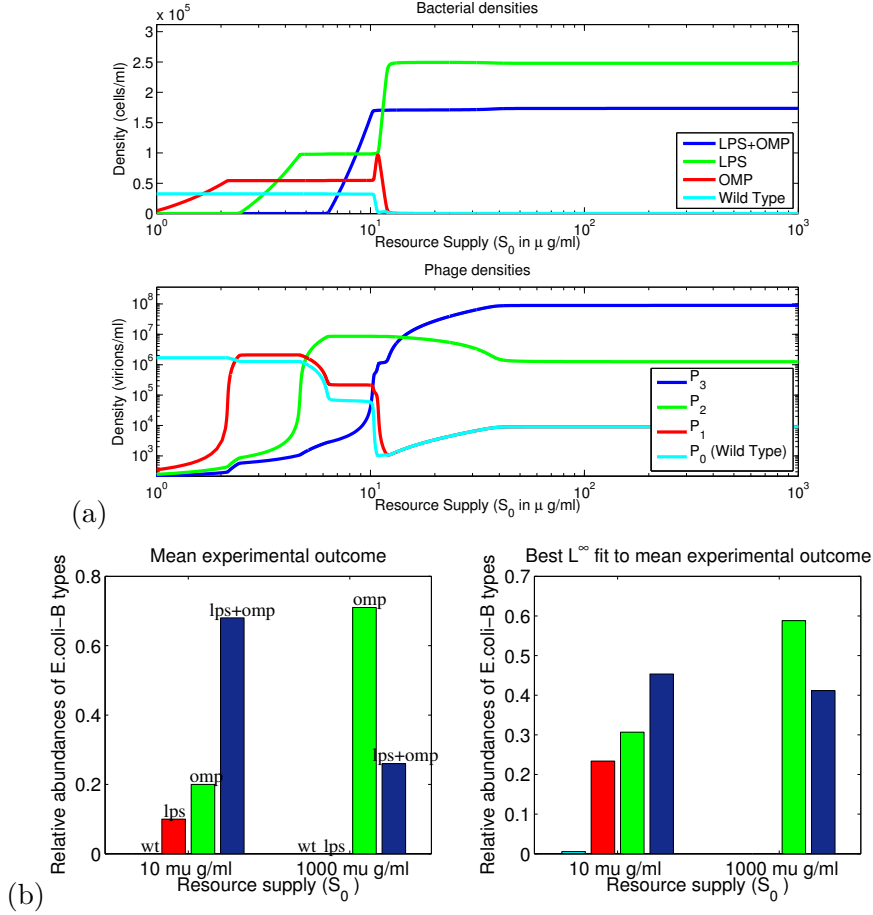


FIGURE 4. (a) Equilibrium densities (per ml) of bacteria and phage mutants showing their dependence on S_0 computed using the parameters given in Table 1 deploying the *modified gene-for-gene* model $\Phi_{mGFG}(\nu, \mu)$ within equation (2). (b) A comparison of experimentally-obtained rank abundances taken from Figure 3, here shown without error bars on the left, with rank abundances found in the model taken from (a) above and shown on the right.

Figure 4 compares the bacterial rank abundances found using model and experiment for two values of the resource supply, namely $S_0 = 10\mu\text{g/ml}$ and $S_0 = 1000\mu\text{g/ml}$. Figure 5 shows the bacterial and phage densities at equilibrium as a function of the resource supply parameter S_0 computed using (2) with the parameters given in Table 1.

We conclude from this comparison that the relative rank abundances of equilibria of the model (2) are consistent with those observed empirically. Figure 4(a) then predicts the experimental rank abundances at all resource concentrations between 1 and 1000 $\mu\text{g/ml}$. There are two clear predictions:

1. the variation in bacterial diversity is greatest for $S_0 < 10\mu\text{g/ml}$, moreover both bacteria and phage diversity eventually *decreases* as S_0 gets sufficiently

large (as seen in Figure 5 where this is demonstrated for two diversity measures).

2. Bacterial diversity is close to a constant value for values of S_0 between 30 and 1000 $\mu\text{g/ml}$.

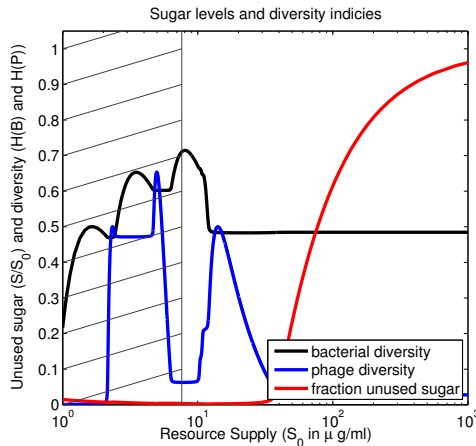


FIGURE 5. Bacteria (black) and phage (blue) diversity patterns are shown for the Shannon-Wiener diversity index here denoted $H(\cdot)$; the variation in diversity is greatest in the hatched region. The fraction of unmetabolised resource, $(S_0 - S)/S_0$, is shown in red.

4. MATHEMATICAL RESULTS

We begin this section with a simple existence and uniqueness result for (2), the purpose of which is to give a point dissipative bound in a weighted norm that will prove useful later. Throughout the remainder we shall assume, unless explicitly stated otherwise, that

$$\mathbf{B}(S) = \boldsymbol{\mu}_{\max} \cdot \Lambda(S) \quad \text{and} \quad \mathbf{U}(S) = \mathbf{V}_{\max} \cdot \Lambda(S),$$

whereby $\boldsymbol{\mu}_{\max} = C \cdot \mathbf{V}_{\max}$. We recall that $\boldsymbol{\mu}_{\max}$ is the maximal growth rate of a cell, \mathbf{V}_{\max} is the maximal resource uptake rate and C is the growth yield. All systemic parameters, ϵ, d and S_0 for example, are all assumed to be positive throughout the remainder, also the mutation processes \mathcal{M} and \mathcal{M}_p are non-negative and irreducible.

We reiterate an earlier remark that from the form of $\Lambda(S)$ it follows that all bacterial genotypes have the same affinity for the limiting resource, moreover they all have the same growth yield parameter, C . This assumption is not necessary and many results can be derived without it, but it helps simplify the following analysis in several places.

Proposition 1. *For each initial datum $(\mathbf{b}(0), \mathbf{p}(0), S(0))$ satisfying $S(0) \geq 0, \mathbf{b}(0) \geq 0$ and $\mathbf{p}(0) \geq 0$, (2) has a unique solution that is strictly positive for $t > 0$. Moreover for each $\delta > 0$ there exists a $t_\delta > 0$ such that*

$$(5) \quad (\mathbf{1}, \mathbf{b}(t)) + \frac{(\mathbf{1}, \mathbf{p}(t))}{\|\boldsymbol{\beta}\|_\infty} + C \cdot S(t) \leq C \cdot (S_0 + \delta)$$

for all $t > t_\delta$.

Proof. Existence and uniqueness of solutions of (2) is standard, their strict positivity follows from the irreducibility assumptions on \mathcal{M} and \mathcal{M}_p and the positivity of $S(t)$ whenever $S(0) \geq 0$ follows from the form of (2c). Let us define

$$\Sigma(t) := S(t) + \frac{1}{C} \left((\mathbf{1}, \mathbf{b}(t)) + \frac{1}{\|\beta\|_\infty} (\mathbf{1}, \mathbf{p}(t)) \right) - S_0$$

and observe that along solutions of (2) there results

$$(6) \quad \frac{d\Sigma}{dt} = -d\Sigma + C^{-1}(\mathbf{b}, \Phi(\beta/\|\beta\|_\infty - 1)\mathbf{p}).$$

Hence $\frac{d\Sigma}{dt} \leq -d\Sigma$ holds for $t > 0$, from where the result follows. \square

The proof of the following simple result is omitted for brevity.

Proposition 2. *Suppose that $\mathbf{b}(t) \rightarrow 0$ as $t \rightarrow \infty$ along a non-negative solution of (2), then $\mathbf{p}(t) \rightarrow 0$ and $S(t) \rightarrow S_0$ as $t \rightarrow \infty$.*

We deduce that no organism can persist in the chemostat if the dilution rate is too large.

Proposition 3. *Suppose that $d > \rho(\mathcal{M} \cdot \text{diag}(\overline{\mathbf{B}}))$ where $\overline{\mathbf{B}}$ is the vector of maximal growth rates defined in assumption B3. Then, for a given non-negative initial datum in (2), there results $\mathbf{b}(t) \rightarrow 0$ as $t \rightarrow \infty$. As a result, $\mathbf{p}(t) \rightarrow 0$ and $S(t) \rightarrow S_0$ as $t \rightarrow \infty$.*

Proof. Define the positive quantity

$$\bar{\rho} := \max_{S \geq 0} \rho(\mathcal{M} \cdot \text{diag}(\mathbf{B}(S))) = \rho(\mathcal{M} \cdot \text{diag}(\overline{\mathbf{B}}))$$

and compute $\frac{d}{dt}(\mathbf{b}, \mathbf{v})$, where $\mathbf{v} \gg \mathbf{0}$ is a solution of $\text{diag}(\overline{\mathbf{B}})\mathcal{M}^T \mathbf{v} = \bar{\rho} \mathbf{v}$. Then

$$\begin{aligned} \frac{d}{dt}(\mathbf{b}, \mathbf{v}) &= (d\mathbf{b}/dt, \mathbf{v}) = (\mathcal{M} \cdot \text{diag}(\mathbf{B}(S))\mathbf{b} - d\mathbf{b} - (\Phi\mathbf{p})\mathbf{b}, \mathbf{v}) \\ &= (\text{diag}(\mathbf{B}(S))\mathcal{M}^T \mathbf{v} - d\mathbf{v}, \mathbf{b}) - ((\Phi\mathbf{p})\mathbf{b}, \mathbf{v}) \\ &< (\text{diag}(\overline{\mathbf{B}})\mathcal{M}^T \mathbf{v} - d\mathbf{v}, \mathbf{b}) = (\text{diag}(\overline{\mathbf{B}})\mathcal{M}^T \mathbf{v} - \bar{\rho}\mathbf{v} + (\bar{\rho} - d)\mathbf{v}, \mathbf{b}) \\ &= (\bar{\rho} - d)(\mathbf{v}, \mathbf{b}). \end{aligned}$$

We deduce that $(\mathbf{b}(t), \mathbf{v}) < e^{(\bar{\rho}-d)t}(\mathbf{b}(0), \mathbf{v})$ so $\mathbf{b}(t) \rightarrow \mathbf{0}$ as $t \rightarrow \infty$ and the result follows from Proposition 2. \square

4.1. Diversity without phage is independent of resource supply. The result stated in Proposition 4 below describes the diversity supported at equilibrium by (2) in the absence of phage. If we first note that the phage-free set $\{(\mathbf{b}, \mathbf{p}, S) \geq (\mathbf{0}, \mathbf{0}, 0) : \mathbf{p} = \mathbf{0}\}$ is invariant for dynamics of (2), this proposition states that the chemostat can, of course, support a non-zero equilibrium population of bacterial cells at a sufficiently low dilution rate d . However, the model predicts that changing the supply of abiotic resource to the chemostat does not change the diversity of bacterial types found at equilibrium.

Proposition 4. (We make the dependence of \mathcal{M} on ϵ explicit for clarity.) If the parameter d is fixed with $d < \rho(\mathcal{M}_\epsilon \cdot \text{diag}(\overline{\mathbf{B}}))$, then there is an $S_0^c(\epsilon, d) > 0$ such that for each $S_0 > S_0^c(\epsilon, d)$,

$$(7a) \quad 0 = \mathcal{M}_\epsilon(\mathbf{B}(S)\mathbf{b}) - d\mathbf{b},$$

$$(7b) \quad 0 = d(S_0 - S) - (\mathbf{U}(S), \mathbf{b}),$$

has a unique, positive solution, (\mathbf{b}, S) . Furthermore, this solution has the following separable decomposition:

$$(8) \quad \mathbf{b} = \lambda(S_0, \epsilon, d) \cdot \mathbf{n}(\epsilon, d) \quad \text{such that} \quad (\mathbf{n}(\epsilon, d), \mathbf{1}) = 1,$$

and $S \equiv S_0^c(\epsilon, d)$ for all $S_0 > S_0^c(\epsilon, d)$.

Here, the scalar λ is a function $\lambda : \mathbb{R} \times (0, 1) \times \mathbb{R} \rightarrow [0, \infty)$ and $\mathbf{n} : (0, 1) \times \mathbb{R} \rightarrow \mathbb{R}^n$ is independent of S_0 , so too is the equilibrium value of S . Moreover, λ is defined by

$$(9) \quad \lambda(S_0, \epsilon, d) = \begin{cases} \frac{d(S_0 - S_0^c(\epsilon, d))}{(\mathbf{n}(\epsilon, d), \mathbf{U}(S_0^c(\epsilon, d)))} & \text{if } S_0 > S_0^c(\epsilon, d), \\ 0 & \text{otherwise.} \end{cases}$$

Thus, λ exhibits affine dependence on S_0 and extends the non-trivial solution branch of (7) into a bifurcation point from the trivial solution that occurs at $S_0 = S_0^c(\epsilon, d)$.

Proof. Let $\mathbf{A}(S) := \mathcal{M}_\epsilon \cdot \text{diag}(\mathbf{B}(S))$, a non-negative and irreducible matrix, and let $r(S) := \rho(\mathbf{A}(S))$ denotes its spectral radius. As the family $\mathbf{A}(S)$ is strictly increasing with respect to S , so too is $r(S)$ and so there is at most one value of S for which $r(S) = d$. By assumption, $\lim_{S \rightarrow \infty} r(S) > d$ and so there is exactly one value of S for which $r(S) = d$, call this $S_0^c(\epsilon, d)$ and let $\mathbf{n} = \mathbf{n}(\epsilon, d)$ be the strictly positive vector that satisfies

$$\mathbf{A}(S_0^c(\epsilon, d))\mathbf{n} = d\mathbf{n}, \quad (\mathbf{1}, \mathbf{n}) = 1.$$

In order to satisfy (7a-b), let $S = S_0^c(\epsilon, d)$ and set $\mathbf{b} = \lambda \cdot \mathbf{n}$. It is clear that (7a) is satisfied for any λ , however (7b) requires

$$d(S_0 - S) = (\mathbf{U}(S), \mathbf{b}) \quad \text{and so} \quad \lambda = \frac{d(S_0 - S)}{(\mathbf{U}(S), \mathbf{n})}$$

which must be non-negative for \mathbf{b} to define a non-negative solution of (7a-b). \square

The prediction in Proposition 4 that biomass scales linearly with S_0 is borne out in practise (see [14, Fig. 1] for *E. coli* limited by glucose) and is used as a test of resource limitation. Of course, the affine relationship between S_0 and biomass cannot hold up to arbitrarily large concentrations of the limiting resource as, eventually, space itself will become limiting. The biological and mathematical ramifications of this observation are well beyond the scope of this article.

From equation (8) in Proposition 4 one immediately obtains the result, one that we state in Theorem 1 below, that the equilibrium diversity of the phage-free subsystem obtained from (2) by setting $\mathbf{p} = \mathbf{0}$ does not depend upon the resource supply S_0 .

Theorem 1. *Let H be any diversity measure and let $\mathbf{b} = \mathbf{b}(S_0, \epsilon)$ represent the vector of bacterial densities of a non-trivial solution locus of (7) with d fixed, then diversity is independent of the resource supply:*

$$\frac{\partial}{\partial S_0} H(\mathbf{b}(S_0, \epsilon)) = 0.$$

Proof. This is an immediate consequence of (8) and the fact that diversity measures are scale-invariant. \square

4.2. Equilibrium Structure of a Chemostat with Phage. Let us state the equilibrium problem of (2) for completeness:

$$(10a) \quad 0 = \mathcal{M}(\mathbf{B}(S)\mathbf{b}) - (\Phi\mathbf{p})\mathbf{b} - d\mathbf{b},$$

$$(10b) \quad 0 = \mathcal{M}_p(\boldsymbol{\beta}(\Phi^T\mathbf{b})\mathbf{p}) - d\mathbf{p},$$

$$(10c) \quad 0 = d(S_0 - S) - (\mathbf{U}(S), \mathbf{b}),$$

where $\mathcal{M} = I + \epsilon(M - I)$ and $\mathcal{M}_p = I + \epsilon(M_p - I)$ for non-negative and irreducible mutation operators M and M_p , both with mutation rate ϵ .

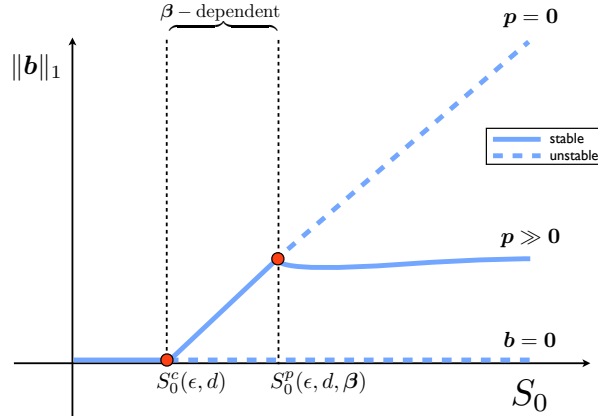


FIGURE 6. An illustration of the equilibrium structure of (2): a unique secondary bifurcation from the phage-free solution branch ($\mathbf{p} = 0$) to a coevolutionary solution branch ($\mathbf{p} \gg 0$).

Theorem 2. *Suppose that Φ is invertible and $0 < d < \rho(\mathcal{M} \cdot \text{diag}(\overline{\mathbf{B}}))$, then there is a second critical resource concentration*

$$S_0^p(\epsilon, d, \boldsymbol{\beta}) > S_0^c(\epsilon, d),$$

where the latter is defined in Proposition 4, such that (10a-c) has at least one solution $(\mathbf{b}, \mathbf{p}, S)$ satisfying $\mathbf{b} \gg \mathbf{0}$, $\mathbf{p} \gg \mathbf{0}$ and $0 < S < S_0$ for all $S_0 > S_0^p(\epsilon, d, \boldsymbol{\beta})$. The resulting solution vector $(\mathbf{b}(S_0), \mathbf{p}(S_0), S(S_0))$ depends smoothly on S_0 and, as $S_0 \downarrow S_0^p(\epsilon, d, \boldsymbol{\beta})$, this vector converges to one of the phage-free form $(\mathbf{b}, \mathbf{0}, S)$.

Moreover, the larger the burst sizes, the smaller the window of resource supply concentrations for which (10a-c) has an equilibrium with bacteria but without phage (see Figure 6):

$$\lim_{\beta \rightarrow \infty, \beta \gg \mathbf{0}} S_0^p(\epsilon, d, \beta) = S_0^c(\epsilon, d).$$

Proof. Although ϵ and d are fixed, we will omit the explicit dependence of the problem on these parameters to reduce notational clutter.

Applying Proposition 4, for $S_0 > S_0^c (= S_0^c(\epsilon, d))$ there is a solution branch of (10) parameterised by the variable S_0 on which

$$(\mathbf{b}, \mathbf{p}, S) = (\lambda(S_0)\mathbf{n}, \mathbf{0}, S_0^c) \quad \text{such that } (\mathbf{1}, \mathbf{n}) = 1,$$

for some vector $\mathbf{n}(= \mathbf{n}(\epsilon, d)) \gg \mathbf{0}$ that is independent of S_0 . We now seek a secondary bifurcation of (10) from this solution branch. For this it will be convenient to distinguish the following irreducible, linear maps

$$(11) \quad \mathbf{A}(S) := \mathcal{M} \cdot \text{diag}(\mathbf{B}(S)),$$

and

$$(12) \quad \mathbf{B}(\mathbf{b}) := \mathcal{M}_p \cdot \text{diag}(\beta) \cdot \text{diag}(\Phi^T \mathbf{b}).$$

By the implicit function theorem, a bifurcation can occur on the phage-free solution branch of (10) only if the linearisation of (10) on this branch has a non-trivial null-space for some $S_0 > S_0^c$. Explicitly, we require a solution of

$$(13a) \quad \mathbf{A}(S_0^c) \mathbf{h} - d\mathbf{h} + \sigma \cdot \lambda(S_0) \mathcal{M} (\mathbf{B}'(S_0^c) \mathbf{n}) - \lambda(S_0) (\Phi \mathbf{k}) \mathbf{n} = \mathbf{0},$$

$$(13b) \quad \lambda(S_0) \mathbf{B}(\mathbf{n}) \mathbf{k} - d\mathbf{k} = \mathbf{0},$$

$$(13c) \quad -(\mathbf{U}(S_0^c), \mathbf{h}) - \sigma \cdot (d + \lambda(S_0) (\mathbf{U}'(S_0^c), \mathbf{n})) = 0$$

for some $(\mathbf{h}, \mathbf{k}, \sigma) \neq (\mathbf{0}, \mathbf{0}, 0)$ where $S_0 > S_0^c$. Here $\mathbf{U}'(S_0^c)$ and $\mathbf{B}'(S_0^c)$ denote S -derivatives of $\mathbf{U}(S)$ and $\mathbf{B}(S)$ evaluated at $S = S_0^c$.

Since $\mathbf{n} \gg \mathbf{0}, \beta \gg \mathbf{0}$, Φ^T is invertible and \mathcal{M}_p is irreducible, $\mathbf{B}(\mathbf{n})$ has a simple, positive and S_0 -independent eigenvalue, $\omega(\epsilon, d, \beta)$, with corresponding strictly-positive left and right eigenvectors that we shall respectively denote by \mathbf{l} and \mathbf{r} . Taking the inner product of (13b) with \mathbf{l} yields the following relation at a secondary bifurcation:

$$(14) \quad \lambda(S_0) \omega(\epsilon, d, \beta) = d.$$

With the restriction from Proposition 4 that $S_0 > S_0^c$, recall the following properties:

$$\lambda(S_0^c) = 0 \text{ and } \lambda(S_0) = \frac{d(S_0 - S_0^c)}{(\mathbf{n}, \mathbf{U}(S_0^c))} \text{ for } S_0 > S_0^c.$$

Viewed as an equation for S_0 , it follows from a simple manipulation that equation (14) has a unique solution that exists when $S_0 > S_0^c$, we label this solution $S_0^p(\epsilon, d, \beta)$ and from a short computation

$$S_0^p = S_0^c + \frac{(\mathbf{n}, \mathbf{U}(S_0^c))}{\omega(\epsilon, d, \beta)}.$$

As $\beta \rightarrow \infty$ with $\beta \geq \underline{\beta} \gg \mathbf{0}$ for some positive vector $\underline{\beta}$, it follows that $\mathbf{B}(\mathbf{n})$ grows without bound and so $\omega(\epsilon, \beta) \rightarrow \infty$ as $\beta \rightarrow \infty$ and therefore $S_0^p \rightarrow S_0^c$ in this limit.

One can see from (10a) evaluated along the phage-free solution branch of (10) (where $\mathbf{p} = \mathbf{0}$) that d is a simple eigenvalue of $\mathbf{A}(S_0^c)$, hence the latter has a corresponding left eigenvector $\mathbf{m} \gg \mathbf{0}$. Given that $\mathbf{k} = \vartheta \mathbf{r}$ for some real ϑ , one can solve (13) for σ by taking the inner product of (13a) with \mathbf{m} to obtain

$$(15) \quad \sigma = \vartheta \cdot \frac{(\mathbf{m}, (\Phi \mathbf{r}) \mathbf{n})}{(\mathbf{m}, \mathcal{M}_\epsilon(\mathbf{B}'(S_0^c) \mathbf{n}))}.$$

Moreover, (13a) can be written

$$(16) \quad (\mathbf{A}(S_0^c) - dI) \mathbf{h} = \mathbf{\Lambda}(\mathbf{k}, \sigma),$$

where $\mathbf{\Lambda}(\mathbf{k}, \sigma) := \lambda(S_0)((\Phi \mathbf{k}) \mathbf{n} - \sigma \cdot \mathcal{M}_\epsilon(\mathbf{B}'(S_0^c) \mathbf{n}))$ is linear in (\mathbf{k}, σ) .

Since $\mathbf{A}(S_0^c) - dI$ has a one-dimensional null-space given by the span of \mathbf{n} , (16) has infinitely many solutions of the form $\mathbf{h} = \vartheta \cdot (\mathbf{h}_p + s\mathbf{n})$, where \mathbf{h}_p is a particular solution of (16), known to exist by the form of σ , and s is any scalar. However, the constant s is uniquely determined using (13c).

We deduce that the linearisation of (10) on the phage-free solution branch has a non-trivial, one-dimensional null-space when $S_0 = S_0^p$, parameterised here by ϑ . As a result, a secondary bifurcation occurs from this branch at $S_0 = S_0^p$, at which point $(\mathbf{b}, \mathbf{p}, S) = (\lambda(S_0^p) \mathbf{n}, \mathbf{0}, S_0^p)$ at which point a non-trivial solution branch bifurcates with $\mathbf{p} \gg \mathbf{0}$. This can be deduced from the theorem on bifurcation from a simple eigenvalue. By standard global extensions of the implicit function theorem, we can extend this branch to one that is defined for all $S_0 > S_0^p$ using the dissipative bound (5) and, from the irreducibility of the mutation processes \mathcal{M} and \mathcal{M}_p , it follows that $\mathbf{b} \gg \mathbf{0}$ and $\mathbf{p} \gg \mathbf{0}$ for all $S_0 > S_0^p$ along this branch. \square

In the remainder we will call the non-trivial solution branch of equilibria whose existence is proven in Theorem 2 the ‘coevolutionary solution branch’ of (2), the semi-trivial branch on which $\mathbf{p} = \mathbf{0}$ will be called the ‘phage-free solution branch’; this bifurcation structure is illustrated in Figure 6.

Lemma 1. *Suppose that Φ is a non-negative, invertible matrix satisfying*

$$\mathbf{p} > \mathbf{0} \implies \Phi \mathbf{p} \gg \mathbf{0}.$$

Then, there is a constant $\bar{m} > 0$ independent of both S_0 and ϵ such that

$$\|\mathbf{b}\|_1 + \|\mathbf{p}\|_1 \leq \bar{m}$$

for any non-negative solution of (10). Consequently, along the coevolutionary solution branch $(\mathbf{b}(S_0), \mathbf{p}(S_0), S(S_0))$ of (10) defined in Theorem 2, there results

$$\lim_{S_0 \rightarrow \infty} S(S_0)/S_0 = 1.$$

Proof. Taking the inner product of (10a) with $\mathbf{1}$, using $\mathcal{M}^T \mathbf{1} = \mathbf{1}$ and the triangle inequality we find $|(\Phi \mathbf{p}, \mathbf{b})| \leq d |(\mathbf{1}, \mathbf{b})| + |(\mathbf{B}(S), \mathbf{b})| \leq d \|\mathbf{1}\|_\infty \|\mathbf{b}\|_1 + \|\mathbf{B}(S)\|_\infty \|\mathbf{b}\|_1$ from where $|(\Phi \mathbf{p}, \mathbf{b} / \|\mathbf{b}\|_1)| \leq d \|\mathbf{1}\|_\infty + \|\mathbf{B}(S)\|_\infty \leq d + \|\overline{\mathbf{B}}\|_\infty$. So, if we define $P := \mathbf{p} / \|\mathbf{p}\|_1$ and $B := \mathbf{b} / \|\mathbf{b}\|_1$ then

$$|(\Phi P, B)| \leq (d + \|\overline{\mathbf{B}}\|_\infty) / \|\mathbf{p}\|_1.$$

If there is a sequence of solutions of (10) along which $\|\mathbf{p}\|_1 \rightarrow \infty$ then we can find non-negative, unit-norm vectors $P > 0$ and $B > 0$ such that $|(\Phi P, B)| = 0$. But as $\Phi P \gg 0$, it must follow that $B = 0$, a contradiction which ensures that $\|\mathbf{p}\|_1$ is uniformly bounded along solutions of (10).

Similarly, taking the inner product of (10b) with $\mathbf{1}$ and using $\mathcal{M}_p^T \mathbf{1} = \mathbf{1}$ we obtain

$$0 = (\mathbf{1}, \mathcal{M}_p (\beta (\Phi^T \mathbf{b}) \mathbf{p}) - d \mathbf{p}) = (\mathbf{1}, \beta (\Phi^T \mathbf{b}) \mathbf{p}) - d(\mathbf{1}, \mathbf{p})$$

so $d(\mathbf{1}, \mathbf{p}) = (\Phi(\beta \mathbf{p}), \mathbf{b})$, therefore $d = (\Phi(\beta P), B)$ and then

$$d / \|\mathbf{b}\|_1 = (\Phi(\beta P), B).$$

Thus, if $\|\mathbf{b}\|_1 \rightarrow \infty$ along a sequence of solutions of (10) then there exist non-negative unit vectors P and B such that $(\Phi(\beta P), B) = 0$. But, by assumption $\Phi(\beta P)$ is a strictly positive vector, a contradiction, and the existence of a uniform bound on both \mathbf{b} and \mathbf{p} now follows.

Finally, because $d(S_0 - S) = (\mathbf{U}(S), \mathbf{b})$ holds at steady-state and $\mathbf{b}(S_0)$ has been shown to be uniformly bounded with respect to S_0 and $\mathbf{U}(S)$ is bounded *a priori*, it follows that

$$d(1 - S/S_0) = (\mathbf{U}(S(S_0)), \mathbf{b}(S_0)) / S_0 \rightarrow 0$$

as $S_0 \rightarrow \infty$. Hence $S(S_0)/S_0 \rightarrow 1$ along the coevolutionary solution branch as claimed. \square

Lemma 1 states that the phage-free branch of (10) behaves differently from the coevolutionary branch: the former diverges in density as $S_0 \rightarrow \infty$ and with constant diversity, however the latter is uniformly bounded in both phage and bacterial densities as the resource supply increases. This embodies the idea that when resource supply is high, the bacteria are limited by phage rather than by the resource. Thus, in chemostats run at high resource concentrations with phage, most of the abiotic resource passes through the chemostat without being metabolised.

4.3. Global convergence to equilibrium. Throughout the paper we have, and will continue to tacitly assume the following: positive solution trajectories of (2) converge to the phage-free equilibrium if $S_0 \in (S_0^c, S_0^p)$ and to the coevolutionary equilibrium if $S_0 > S_0^p$. This assumption can be verified for some important but, unfortunately, not exhaustive classes of the model. While extensive numerical simulation has not led to any reason to believe such a global stability assumption fails, we acknowledge that it yet may.

It remains an important caveat of the results in this paper that equilibrium diversity can be used to describe the long-term diversity of solutions of (2) and in relation to this remark, we note that certain global convergence results are available, as illustrated by the following.

Suppose that $\mathcal{M} = I + (M - I)\mathcal{E}$ is an irreducible mutation process with diagonal mutation rate matrix \mathcal{E} , that $\mu_0 > 0, K_0 > 0, \boldsymbol{\mu} = (\mu_1, \dots, \mu_n) \in \mathbb{R}^n$ and $\mathbf{K} = (K_1, \dots, K_n) \in \mathbb{R}^n$ are all positive but otherwise arbitrary. Now define a growth yield parameter $C > 0$. Using these parameters, define Michaelis-Menten growth functions

$$B_i(S, \vartheta) := \frac{S(\mu_0 + \vartheta\mu_i)}{S + (K_0 + \vartheta K_i)}, \quad i = 1, 2, \dots, n,$$

and set their associated uptake rates to be $U_i(S, \vartheta) := C^{-1} \cdot B_i(S, \vartheta)$. A vector of Michaelis-Menten growth function

$$\mathbf{B}_\vartheta(S) := (B_1(S, \vartheta), B_2(S, \vartheta), \dots, B_n(S, \vartheta))$$

can now be defined that satisfies assumptions (B1-B3) for fixed $\vartheta > 0$, now set $\mathbf{U}_\vartheta(S) := C^{-1} \mathbf{B}_\vartheta(S)$.

Finally, fix a single burst rate $\beta > 0$ and create a vector of adsorption rates $\phi_\vartheta := \mathbf{1} + \vartheta \cdot \phi'$ of each of the n bacterial types to just *one* phage type, where ϕ' is any $n \times 1$ vector.

Theorem 3. *Consider the following bacteria-phage model:*

$$(17a) \quad \frac{d\mathbf{b}}{dt} = \mathcal{M}(\mathbf{B}_\vartheta(S)\mathbf{b}) - d\mathbf{b} - p \cdot \text{diag}(\phi_\vartheta)\mathbf{b}, \quad \in \mathbb{R}^n$$

$$(17b) \quad \frac{dp}{dt} = \beta(\phi_\vartheta^T \mathbf{b})p - dp, \quad \in \mathbb{R}^1$$

$$(17c) \quad \frac{dS}{dt} = d(S_0 - S) - (\mathbf{U}_\vartheta(S), \mathbf{b}).$$

Suppose that $S_0 > 0$ and $d > 0$ are fixed and that and all equilibria of (17) are hyperbolic when $\vartheta = 0$. Then there is a $\delta > 0$ such that for $0 \leq \vartheta < \delta$, all non-negative solution trajectories of (17) are attracted to an equilibrium as $t \rightarrow \infty$.

Proof. First note that

$$\mathbf{U}_0(S) = \frac{1}{C} \cdot \frac{\mu_0 S}{K_0 + S} \cdot \mathbf{1}, \quad \mathbf{B}_0(S) = \frac{\mu_0 S}{K_0 + S} \cdot \mathbf{1} \quad \text{and} \quad \text{diag}(\phi_0) = I$$

when $\vartheta = 0$.

Exploiting the dissipativity of (17) proven in Proposition 1, we deduce that along any non-negative solution of (17), $(\mathbf{b}(t), p(t), S(t))$, there is a $t' > 0$ such that

$$(18) \quad (\mathbf{1}, \mathbf{b}(t)) + p(t)/\beta + C \cdot S(t) \leq C \cdot (S_0 + 1)$$

for all $t > t'$.

We first prove that the dynamics of (17) are attracted to a long-term equilibrium when $\vartheta = 0$, as follows. Using the irreducibility of \mathcal{M} , the decomposition

$$\mathbf{b}(t) = \alpha(t)(\boldsymbol{\nu} + \mathbf{v}(t)) \in \langle \boldsymbol{\nu} \rangle \oplus \langle \mathbf{1} \rangle^\perp, \quad \alpha(t) \in \mathbb{R},$$

is well-defined, where $\mathcal{M}\boldsymbol{\nu} = \boldsymbol{\nu}$, $(\mathbf{1}, \boldsymbol{v}(t)) \equiv 0$ and $(\mathbf{1}, \boldsymbol{\nu}) = 1$.

As $\dot{\boldsymbol{b}}(t) = \dot{\alpha}(t)(\boldsymbol{\nu} + \boldsymbol{v}(t)) + \alpha(t)\dot{\boldsymbol{v}}(t)$, the fact that $\vartheta = 0$ leads to a good deal of simplification in a calculation that eventually yields, in place of (17a), the following pair of differential equations:

$$\dot{\boldsymbol{v}} = \frac{\mu_0 S}{K + S} (\mathcal{M} - I) \boldsymbol{v}, \quad \dot{\alpha} = \alpha \left(\frac{\mu_0 S}{K + S} - d - p \right), \quad \boldsymbol{v} \in \langle \mathbf{1} \rangle^\perp.$$

From here we calculate

$$\frac{d}{dt}(\boldsymbol{v}, \boldsymbol{v}) = 2(\dot{\boldsymbol{v}}, \boldsymbol{v}) = 2 \frac{\mu_0 S}{K + S} ((\mathcal{M} - I) \boldsymbol{v}, \boldsymbol{v}).$$

From the assumption stated in (1) that $\mathcal{M} - I$ is strictly negative definite when restricted to its invariant space $\langle \mathbf{1} \rangle^\perp$, we deduce that

$$\frac{d}{dt}(\boldsymbol{v}, \boldsymbol{v}) \leq 2\mu_0 \left(\sup_{\boldsymbol{v} \in \langle \mathbf{1} \rangle^\perp, \|\boldsymbol{v}\|_2=1} ((\mathcal{M} - I) \boldsymbol{v}, \boldsymbol{v}) \right) \cdot (\boldsymbol{v}, \boldsymbol{v}) = -2\mu_0 \rho_0 \cdot (\boldsymbol{v}, \boldsymbol{v}).$$

Integrating this inequality yields $\|\boldsymbol{v}(t)\|_2 \leq e^{-\rho_0 \mu_0 t} \|\boldsymbol{v}(0)\|_2$ where $\rho_0 > 0$ and $\mu_0 > 0$. As $\boldsymbol{v}(t)$ therefore converges exponentially to zero, (17) has an exponentially attracting invariant set on which $\boldsymbol{v} = \mathbf{0}$ when $\vartheta = 0$ and so (17) then reduces to the three-dimensional system

$$(19a) \quad \frac{d\alpha}{dt} = \alpha \left(\frac{\mu_0 S}{K + S} - d - p \right),$$

$$(19b) \quad \frac{dp}{dt} = \beta \alpha p - dp,$$

$$(19c) \quad \frac{dS}{dt} = d(S_0 - S) - \alpha (\mathbf{U}_0(S), \boldsymbol{\nu}).$$

If we define $\Sigma = S_0 - S - C^{-1}(\alpha + \beta^{-1}p)$, then $\dot{\Sigma} = -d\Sigma$ along solutions of (19) and so (19) is dissipative, as it must be. But then the set on which $\Sigma = 0$ defines an exponentially-attracting invariant manifold of (19) on which $C \cdot S + \alpha + p/\beta = C \cdot S_0$ so that one may write $S = S(\alpha, p) := S_0 - (\alpha + p/\beta)/C$ on this invariant set.

If we now define $A = \ln(\alpha)$ and $P = \ln(p)$ then (19) has periodic solutions for non-negative initial data if and only if the planar system

$$(20a) \quad \frac{dA}{dt} = \frac{\mu_0 S(e^A, e^P)}{K + S(e^A, e^P)} - d - e^P,$$

$$(20b) \quad \frac{dP}{dt} = \beta e^A - d,$$

also supports an appropriate period solution. The divergence of the vector field that defines (20) is sign-definite and so this differential equation has no periodic orbits, but then neither does (19). As (19) is dissipative with an attracting, invariant two-dimensional affine graph and it defines a dynamical system on this graph with no periodic orbits, we conclude that the long-term behaviour of trajectories of (19) is to converge to a steady-state by the Poincaré-Bendixson theorem.

As (19) only has three possible equilibria, where $\alpha = p = 0$, one where $p = 0$ but $\alpha > 0$ and one where both $\alpha > 0, p > 0$, exactly which equilibria exist depends upon

the system parameters. However, provided those parameters are chosen in such a way that all of the equilibria are hyperbolic, because only one of them can be locally stable for any set of parameter values, the one that is both hyperbolic and locally stable is also globally stable for (17) for a generic choice of non-negative initial data.

Now applying [31, Corollary 2.3], one can readily prove that this global stability property persists to small, positive values of the parameter ϑ . \square

Theorem 3 is but one of a family of similar results and this particular result describes a situation in which there is just one phage type. There are straightforward extensions in a number of directions, including ones to systems with multiple phage types.

5. RESOURCE-MEDIATED DIVERSITY: AN EXACTLY SOLVABLE MODEL

We now in a position to return the original question of what patterns of diversity, such as that shown in Figure 5, are generated by (10) when one fixes all other parameters but varies the resource concentration supplied to the chemostat. Figure 5 shows that bacterial diversity is constant for high values of S_0 and that phage diversity is maximal at ‘intermediate’ values of S_0 ; but is this the only pattern of diversity predicted by (2)?

We assume the following throughout this section: Φ will be a non-singular matrix with

$$(21) \quad \Phi^{-1}(\bar{\mathbf{B}} - d\mathbf{1}) \gg \mathbf{0} \quad \text{and} \quad \Phi^{-T}(\mathbf{1}/\boldsymbol{\beta}) \gg \mathbf{0}.$$

For technical reasons, it is also important to note that there exists a $\hat{\mathbf{B}} \in \mathbb{R}^n$ such that

$$\lim_{S \rightarrow \infty} S^2 \cdot \frac{d\mathbf{B}}{dS}(S) = \hat{\mathbf{B}}.$$

One limitation regarding the applicability of condition (21) is the assumption that Φ^{-1} maps certain positive vectors to positive vectors. This will occur quite generally if Φ^{-1} is a non-negative matrix, but this is too strong an assumption to use in general as it places severe restrictions on the form Φ can take.

However, the conditions in (21) are indeed relevant to adsorption matrices found in the literature. For example, if we define a gene-for-gene interaction between four genetically distinct bacterial and phage types with burst sizes $\boldsymbol{\beta}$ and if

$$\Phi = \theta \cdot \begin{bmatrix} a & b & c & d \\ 0 & e & 0 & g \\ 0 & 0 & h & k \\ 0 & 0 & 0 & 1 \end{bmatrix} \quad \text{and} \quad \boldsymbol{\beta} = \|\boldsymbol{\beta}\|_{\infty} \cdot \begin{pmatrix} 1/u \\ 1/v \\ 1/w \\ 1 \end{pmatrix},$$

(21) would then require positivity of the vector

$$\Phi^{-1}(\mathbf{1}/\boldsymbol{\beta}) = \frac{\|\boldsymbol{\beta}\|_{\infty}}{\theta} \begin{bmatrix} \frac{u}{a} - \frac{bv}{ea} - \frac{cw}{ha} + \frac{bgh+cke-deh}{aeh} \\ (v-g)/e \\ (w-k)/h \\ 1 \end{bmatrix}.$$

This condition clearly depends on the parameters contained within Φ and $\boldsymbol{\beta}$, however, there are many parameter values for which (21) is met.

Our aim now is to establish the following result regarding the diversity of phage supported by (10) when measured using Simpson's index, H_s .

Theorem 4. *Suppose that d is fixed with $0 < d < \rho(\mathcal{M} \cdot \text{diag}(\overline{\mathbf{B}}))$ and $\epsilon > 0$ is fixed. Then, there is an $S_0^v > 0$ and a function $\mathbf{v} : (S_0^v, \infty) \rightarrow \mathbb{R}^n$ such that the coevolutionary solution branch $(\mathbf{b}(S_0, \epsilon), \mathbf{p}(S_0, \epsilon), S(S_0, \epsilon))$ of (10) satisfies*

$$\|\mathbf{p}(S_0, \epsilon) - \mathbf{v}(S_0)\| = O(\epsilon)$$

as $\epsilon \searrow 0$ uniformly for $S_0 > S_0^v$. Moreover, one of only two possibilities occurs, either

- (i). $\frac{d}{dS_0} H_s(\mathbf{v}(S_0)) \neq 0$ for all $S_0 > S_0^v$ or
- (ii). there is a unique $S_0 > S_0^v$ such that $\frac{d}{dS_0} H_s(\mathbf{v}(S_0)) = 0$.

Within the same range of values of S_0 , equilibrium bacterial diversity $H_s(\mathbf{b}(S_0, \epsilon))$ is $O(\epsilon)$ -close to a constant function.

Theorem 4 states that the restrictions on the model (10) assumed in this paper permit two outcomes: the equilibrium diversity of phage is $O(\epsilon)$ -close to a function that is either unimodal or monotonic in resource supply and the equilibrium diversity of bacteria is $O(\epsilon)$ -close to a constant. In short, diversity of neither phage nor bacteria can *oscillate* as S_0 grows.

We shall prove Theorem 4 with a series of lemmas that now follow.

Lemma 2. *Consider the ecological equilibrium equations obtained by setting $\epsilon = 0$ in (10), namely*

$$(22a) \quad 0 = \mathbf{B}(S)\mathbf{b} - (\Phi\mathbf{p})\mathbf{b} - d\mathbf{b},$$

$$(22b) \quad 0 = \boldsymbol{\beta}(\Phi^T\mathbf{b})\mathbf{p} - d\mathbf{p},$$

$$(22c) \quad 0 = d(S_0 - S) - (\mathbf{U}(S), \mathbf{b}).$$

There is an interval $(S_0^v, \infty) \subset \mathbb{R}$ and a smooth function $S : (S_0^v, \infty) \rightarrow \mathbb{R}^{n+n+1}$ that parameterises a unique, strictly positive solution branch of (22) as a function of S_0 . Moreover, on this branch there results

$$\mathbf{b}(S_0) \equiv d\Phi^{-T}(\mathbf{1}/\boldsymbol{\beta}) \quad \text{and} \quad \mathbf{p}(S_0) = \Phi^{-1}(\mathbf{B}(S(S_0)) - d\mathbf{1})$$

where the function $S(S_0)$ satisfies

$$S(S_0) = S_0 - (\mathbf{V}_{\max}, \Phi^{-T}(\mathbf{1}/\boldsymbol{\beta})) + O(S_0^{-1})$$

as $S_0 \rightarrow \infty$.

Proof. From the conditions in (21), equation (22) has the following analytic solution:

$$\mathbf{b} \equiv d\Phi^{-T}(\mathbf{1}/\beta) \quad \text{and} \quad \mathbf{p} = \Phi^{-1}(\mathbf{B}(S) - d\mathbf{1})$$

where $d(S_0 - S) = (\mathbf{U}(S), \mathbf{b})$ and so

$$(23) \quad S_0 = S + \Lambda(S)(\mathbf{V}_{\max}, \Phi^{-T}(\mathbf{1}/\beta)) = S + \frac{S}{K + S}(\mathbf{V}_{\max}, \Phi^{-T}(\mathbf{1}/\beta)).$$

Equation (23) can be written as a quadratic in S that may be solved for S as a function of S_0 , thus completing the proof. \square

In order to incorporate mutations into Lemma 2 but at a low rate, we turn to the coevolutionary steady state equation (10).

Lemma 3. *There is a set $\Omega := (\overline{S_0}, \infty) \times [0, \bar{\epsilon})$ and a unique function $(\mathbf{b}, \mathbf{p}, S) : \Omega \rightarrow \mathbb{R}^{n+n+1}$ that parameterises the family of unique positive solutions of (10) such that*

$$(24) \quad \mathbf{b}(S_0, \epsilon) = d\Phi^{-T}(\mathbf{1}/\beta) + \epsilon E_b(\epsilon, S_0^{-1}), \quad \mathbf{p}(S_0, \epsilon) = \Phi^{-1}(\mathbf{B}(S) - d\mathbf{1}) + \epsilon E_p(\epsilon, S_0^{-1}),$$

where

$$S(S_0, \epsilon) = S_0 - (\mathbf{V}_{\max}, \Phi^{-T}(\mathbf{1}/\beta)) + O(S_0^{-1}) + \epsilon E_s(\epsilon, S_0^{-1})$$

and E_b, E_p, E_s are smooth functions of their arguments.

Proof. Put $\delta := 1/S, \sigma := S_0/S$ and define $\tilde{\mathbf{B}}(\delta) := \mathbf{B}(S)$ in (10), giving the relation

$$(25a) \quad 0 = \mathcal{M}_\epsilon(\tilde{\mathbf{B}}(\delta)\mathbf{b}) - (\Phi\mathbf{p})\mathbf{b} - d\mathbf{b}$$

that replaces (10a). Now desingularise $\tilde{\mathbf{B}}(\delta)$ at $\delta = 0$ by defining $\tilde{\mathbf{B}}(0) := \lim_{S \rightarrow \infty} \mathbf{B}(S) = \overline{\mathbf{B}} \gg \mathbf{0}$ and

$$\left. \frac{d}{d\delta} \tilde{\mathbf{B}}(\delta) \right|_{\delta=0} := \lim_{S \rightarrow \infty} -\mathbf{B}'(S)S^2 = -\hat{\mathbf{B}}.$$

Note that (10c) can be written in terms of δ as

$$(25b) \quad 0 = d(\sigma - 1) - \delta \left(\tilde{\mathbf{U}}(\delta), \mathbf{b} \right),$$

after defining and then desingularising the vector of uptake rates $\tilde{\mathbf{U}}(\delta) := \mathbf{U}(S)$.

To solve the new system of desingularised equations (25a, 25b, 10b), let the right-hand side of this set of three equations be denoted by the smooth, nonlinear mapping $\mathcal{F}(\mathbf{b}, \mathbf{p}, \sigma, \delta, \epsilon)$, noting that

$$(\mathbf{b}_0, \mathbf{p}_0, \sigma_0, \delta_0, \epsilon_0) := (d\Phi^{-T}(\mathbf{1}/\beta), \Phi^{-1}(\overline{\mathbf{B}} - d\mathbf{1}), 1, 0, 0)$$

is a solution of $\mathcal{F}(\mathbf{b}, \mathbf{p}, \sigma, \delta, \epsilon) = \mathbf{0}$. The derivative $d_{\mathbf{b}, \mathbf{p}, \sigma} \mathcal{F}(\mathbf{b}, \mathbf{p}, \sigma, \delta, \epsilon)$ is given by the mapping

$$(26) \quad \begin{aligned} \mathcal{L}(\mathbf{b}, \mathbf{p}, \sigma, \delta, \epsilon) [\mathbf{h}, \mathbf{k}, s] &:= \left[\mathcal{M}(\tilde{\mathbf{B}}(\delta))\mathbf{h} - (\Phi\mathbf{p})\mathbf{h} - d\mathbf{h} - (\Phi\mathbf{k})\mathbf{b}, \right. \\ &\left. \mathcal{M}_p(\beta(\Phi^T\mathbf{h})\mathbf{p} + \beta(\Phi^T\mathbf{b})\mathbf{k}) - d\mathbf{k}, -\delta(\mathbf{h}, \tilde{\mathbf{U}}(\delta)) + ds \right]. \end{aligned}$$

As a result, if $\mathcal{L}(\mathbf{b}_0, \mathbf{p}_0, \sigma_0, \delta_0, \epsilon_0) [\mathbf{h}, \mathbf{k}, s] = (\mathbf{0}, \mathbf{0}, 0)$ then $s = 0$ follows because $\delta_0 = 0$ and $d > 0$, but then $\beta(\Phi^T\mathbf{h})\mathbf{p}_0 = 0$ because of the form of \mathbf{b}_0 , whence $\mathbf{h} = \mathbf{0}$

because $\mathbf{p}_0 \gg \mathbf{0}$. From here $(\Phi \mathbf{k}) \mathbf{b}_0 = \mathbf{0}$ and so we deduce that $\mathbf{k} = \mathbf{0}$ because $\mathbf{b}_0 \gg \mathbf{0}$. Hence we can smoothly solve the nonlinear equation $\mathcal{F}(\mathbf{b}, \mathbf{p}, \sigma, \delta, \epsilon) = \mathbf{0}$ for $(\mathbf{b}, \mathbf{p}, \sigma)$ as a function of (δ, ϵ) in a neighbourhood of $(\delta, \epsilon) = (0, 0)$ using the implicit function theorem and this neighbourhood can be used to define Ω .

The Taylor expansions in the statement of the lemma can be established by observing that, when setting $\epsilon = 0$ in (10), the form of the resulting solution is then given by Lemma 2 and the inclusion of mutations induces an $O(\epsilon)$ correction to that form. \square

Remark 2. *In the remainder we will use the notation*

$$(27) \quad \mathbf{w}(S) := \Phi^{-1}(\mathbf{B}(S) - d\mathbf{1}),$$

so that the function $\mathbf{v}(S_0)$ given in Theorem 4 may also be written as $\mathbf{w}(S(S_0))$ where $S(S_0)$ is the value of the resource concentration at steady-state determined from solutions of (22) in Lemma 2. For completeness we note that this function is given by a solution, S , of the quadratic equation

$$S^2 + S((\mathbf{V}_{\max}, \Phi^{-T}(\mathbf{1}/\beta)) - S_0 + K) - KS_0 = 0.$$

The following lemma states that the resource availability S in the environment as measured using solutions of (22) increases with the resource supply parameter S_0 , provided the latter is sufficiently large.

Lemma 4. *For the smoothly-parameterised equilibrium solution branch of (22) defined in Lemma 2, there results $dS/dS_0 > 0$ for $S_0 > S_0^v$.*

Proof. Differentiating (22c) with respect to S_0 we obtain

$$d \left(1 - \frac{dS}{dS_0} \right) = (\mathbf{U}'(S), \mathbf{b}) \frac{dS}{dS_0}$$

where a prime ($'$) denotes a derivative with respect to S , the result now follows. \square

Let us turn to the computation of the S_0 -derivative of phage diversity, $\frac{d}{dS_0} \mathbf{H}_s(\mathbf{v}(S_0))$ which equals $\frac{d}{dS_0} \mathbf{H}_s(\mathbf{w}(S(S_0)))$ and for this purpose we define

$$\mathbf{q}(S) := \mathbf{w}(S)/(\mathbf{1}, \mathbf{w}(S)).$$

Now recall that $\mathbf{H}_s(\mathbf{v}) = 1 - (\mathbf{v}, \mathbf{v})/(\mathbf{1}, \mathbf{v})^2$ so that $\mathbf{H}_s(\mathbf{q}(S)) = 1 - (\mathbf{q}(S), \mathbf{q}(S))$.

If we set $\mathbf{w}'(S) := \frac{d\mathbf{w}}{dS}(S)$, which equals $\Phi^{-1}(\mathbf{B}'(S))$ where $\mathbf{B}'(S) := \frac{d\mathbf{B}}{dS}(S)$, then $H_s(\mathbf{w}(S)) = H_s(\mathbf{q}(S))$ and so

$$\begin{aligned}
\frac{d}{dS_0} H_s(\mathbf{v}(S_0)) &= \frac{d}{dS_0} H_s(\mathbf{w}(S(S_0))), \\
&= \frac{d}{dS_0} H_s(\mathbf{q}(S(S_0))), \\
&= -\frac{d}{dS_0} (\mathbf{q}(S(S_0)), \mathbf{q}(S(S_0))), \\
&= -2 \left(\frac{d\mathbf{q}}{dS}(S(S_0)), \mathbf{q}(S(S_0)) \right) \cdot \frac{dS}{dS_0}, \\
(28) \qquad &= -2(\mathbf{1}, \mathbf{w}(S))^{-3} ((\mathbf{w}, \mathbf{w}')(\mathbf{1}, \mathbf{w}) - (\mathbf{w}, \mathbf{w})(\mathbf{1}, \mathbf{w}')) \cdot \frac{dS}{dS_0}.
\end{aligned}$$

Thus, $\frac{d}{dS_0} H_s(\mathbf{v}(S_0)) = 0$ only when

$$(29) \quad (\mathbf{w}(S), \mathbf{w}'(S))(\mathbf{1}, \mathbf{w}(S)) = (\mathbf{w}(S), \mathbf{w}(S))(\mathbf{1}, \mathbf{w}'(S)), \quad \text{where } S = S(S_0).$$

Recall the notation used here: $\mathbf{U}(S) = \Lambda(S) \cdot \mathbf{V}_{\max}$ and $\mathbf{B}(S) = \Lambda(S) \cdot \boldsymbol{\mu}_{\max}$. The following result completes the proof of Theorem 4.

Lemma 5. *There is at most one value of S_0 at which equation (29) can be satisfied.*

Proof. Equation (29) simplifies somewhat when we note that $\mathbf{w}(S) = \Lambda(S)\mathbf{c} + \mathbf{d}$ for two fixed vectors

$$\mathbf{c} := \Phi^{-1}(\boldsymbol{\mu}_{\max}) \quad \text{and} \quad \mathbf{d} := -d\Phi^{-1}(\mathbf{1}).$$

Thus (29) can be written in terms of $\Lambda(S)$, namely

$$(30) \quad \Lambda'(S) [(\Lambda(S)\mathbf{c} + \mathbf{d}, \mathbf{c})(\mathbf{1}, \Lambda(S)\mathbf{c} + \mathbf{d}) - (\Lambda(S)\mathbf{c} + \mathbf{d}, \Lambda(S)\mathbf{c} + \mathbf{d})(\mathbf{1}, \mathbf{c})] = 0,$$

where $\Lambda'(S) > 0$ for all S . From (30) we obtain the value of S at which diversity is extremal and a straightforward manipulation gives the relation

$$(31) \quad \Lambda(S) = \frac{(\mathbf{d}, \mathbf{d})(\mathbf{1}, \mathbf{c}) - (\mathbf{1}, \mathbf{d})(\mathbf{d}, \mathbf{c})}{(\mathbf{c}, \mathbf{c})(\mathbf{1}, \mathbf{d}) - (\mathbf{c}, \mathbf{d})(\mathbf{1}, \mathbf{c})}.$$

As $\Lambda(S)$ depends monotonically on S and S depends monotonically on S_0 for $S_0 > S_0^v$, there is at most one value of S_0 at which equation (31) can be satisfied and the result follows. \square

We are now in a position to ask whether different *patterns of diversity* may be generated by (10) as S_0 changes. The first statement in this direction is the following result which shows that if the adsorption matrix has a structure whereby the **total** adsorption rate of each phage type to each bacterial type is the same, then phage diversity must eventually *increase* as S_0 increases.

Proposition 5. *Suppose that $\Phi(\mathbf{1}) = \alpha\mathbf{1}$ where α is an algebraically simple eigenvalue of Φ . If $\mathbf{V}_{\max} \notin \langle \mathbf{1} \rangle$, then only case (i) of Theorem 4 can occur and phage diversity increases with resource concentration in the sense that*

$$\frac{d}{dS_0} H_s(\mathbf{v}(S_0)) > 0$$

for $S_0 > S_0^v$.

Proof. If we again define $\mathbf{c} := \Phi^{-1}(\boldsymbol{\mu}_{\max})$ and $\mathbf{d} := -d\Phi^{-1}(\mathbf{1})$, then $\boldsymbol{\mu}_{\max} = C \cdot \mathbf{V}_{\max}$ and because $\mathbf{V}_{\max} \notin \langle \mathbf{1} \rangle$, $\boldsymbol{\mu}_{\max} \notin \langle \mathbf{1} \rangle$ is also true. The assumptions on Φ then ensure that $\mathbf{c} \notin \langle \mathbf{1} \rangle$ and so $|\langle \mathbf{c}, \mathbf{1} \rangle| < \|\mathbf{1}\|_2 \|\mathbf{c}\|_2$ holds strictly from the Cauchy-Schwartz inequality.

Recall that $\mathbf{w}(S) = \Lambda(S)\mathbf{c} + \mathbf{d}$, so $\mathbf{w}'(S) = \Lambda'(S)\mathbf{c}$ which is positive for $S > 0$. Seeking an *extreme diversity environment*, namely a value of S for which (31) holds, we find, because $\Phi(\mathbf{1}) = \alpha\mathbf{1}$ that $\mathbf{d} = -d\Phi^{-1}(\mathbf{1}) = -(d/\alpha)\mathbf{1}$. Hence

$$\begin{aligned} \Lambda(S) &= \frac{(-d\alpha^{-1}\mathbf{1}, -d\alpha^{-1}\mathbf{1})(\mathbf{1}, \mathbf{c}) - (\mathbf{1}, -d\alpha^{-1}\mathbf{1})(-d\alpha^{-1}\mathbf{1}, \mathbf{c})}{(\mathbf{c}, \mathbf{c})(\mathbf{1}, -d\alpha^{-1}\mathbf{1}) - (\mathbf{c}, -d\alpha^{-1}\mathbf{1})(\mathbf{1}, \mathbf{c})} \\ &= 0 / (-d\alpha^{-1}(\mathbf{c}, \mathbf{c})(\mathbf{1}, \mathbf{1}) + d\alpha^{-1}(\mathbf{c}, \mathbf{1})(\mathbf{1}, \mathbf{c})) = 0 \end{aligned}$$

which is well-defined as $(\mathbf{c}, \mathbf{c})(\mathbf{1}, \mathbf{1}) \neq (\mathbf{c}, \mathbf{1})^2$. However, $\Lambda(S)$ does not equal zero unless $S = 0$ and so the extreme diversity equation (29) cannot be satisfied for $S > 0$.

From (28), recalling $\mathbf{q}(S) = \mathbf{w}(S) / (\mathbf{1}, \mathbf{w}(S))$ and $\mathbf{w}(S) = \Lambda(S)\mathbf{c} + \mathbf{d}$, we have

$$\frac{d}{dS_0} H_s(\mathbf{q}(S(S_0))) = -2(\mathbf{1}, \mathbf{w}(S))^{-3} ((\mathbf{w}, \mathbf{w}')(\mathbf{1}, \mathbf{w}) - (\mathbf{w}, \mathbf{w})(\mathbf{1}, \mathbf{w}')) \cdot \frac{dS}{dS_0}$$

evaluated at $S = S_0$, and, from Lemma 4,

$$\text{sign} \left(\frac{d}{dS_0} H_s(\mathbf{q}(S(S_0))) \right) = -\text{sign} ((\mathbf{w}, \mathbf{w}')(\mathbf{1}, \mathbf{w}) - (\mathbf{w}, \mathbf{w})(\mathbf{1}, \mathbf{w}')) .$$

A straightforward calculation now shows that

$$(\mathbf{w}, \mathbf{w}')(\mathbf{1}, \mathbf{w}) - (\mathbf{w}, \mathbf{w})(\mathbf{1}, \mathbf{w}') = d\Lambda(S)\Lambda'(S) \cdot ((\mathbf{c}, \mathbf{1})^2 - (\mathbf{c}, \mathbf{c})(\mathbf{1}, \mathbf{1}))$$

which is negative from the Cauchy-Schwartz inequality and the result follows. \square

6. WHEN DIVERSITY INCREASES WITH RESOURCE AVAILABILITY

The experimental data and associated mathematical model whose results we summarised in Figure 4 show that bacterial and phage diversity may *decrease* as sugar supply to the microcosm increases. However, the analysis of the previous section shows that there is at least one other possible outcome even in a model as simple as the one stated in equation (2).

Proposition 5 provides a condition under which the equilibrium diversity of phage obtained using (10) will be $O(\epsilon)$ -close to a monotonic *increasing* function for large enough S_0 . This *uniform adsorption condition* which states that

$$(32) \quad \Phi(\mathbf{1}) = \alpha\mathbf{1},$$

although restrictive, has several biological interpretations.

For example, it expresses the idea of an adsorption trade-off in the sense that bacteria that are susceptible to a lower number of phage types have higher probabilities of infection by each of those phage types. Equivalently, phage types with wider host ranges have lower probabilities of adsorption to each single bacterial type. So, for example, Proposition 5 may apply if

$$\Phi = \theta \cdot \begin{bmatrix} \frac{1}{4} & \frac{1}{4} & \frac{1}{4} & \frac{1}{4} \\ 0 & \frac{1}{3} & \frac{1}{3} & \frac{1}{3} \\ 0 & 0 & \frac{1}{2} & \frac{1}{2} \\ 0 & 0 & 0 & 1 \end{bmatrix},$$

which incorporates the trade-off property that phage with wider host ranges have lower per-host adsorption rates.

Another interpretation comes from the idea of a *perfect lock and key* or a *perfectly matching alleles* mechanism between phage and their bacterial hosts. This is where Φ is proportional to an identity matrix, $\Phi = \theta I$, for some $\theta > 0$, meaning that each phage type has a single bacterial host type to which it adsorbs, but no other.

Example 1. *If the adsorption mechanism in (10) is the matching-alleles structure whereby $\Phi = \theta I$ then Proposition 5 may be applied. We deduce that phage diversity at equilibrium, modulo an $O(\epsilon)$ correction, will eventually increase with resource supply. Figure 7 contains a numerically-computed illustration of this adsorption model where the positive correlation between S_0 and phage diversity is evident (see Figure 7(b) in particular).*

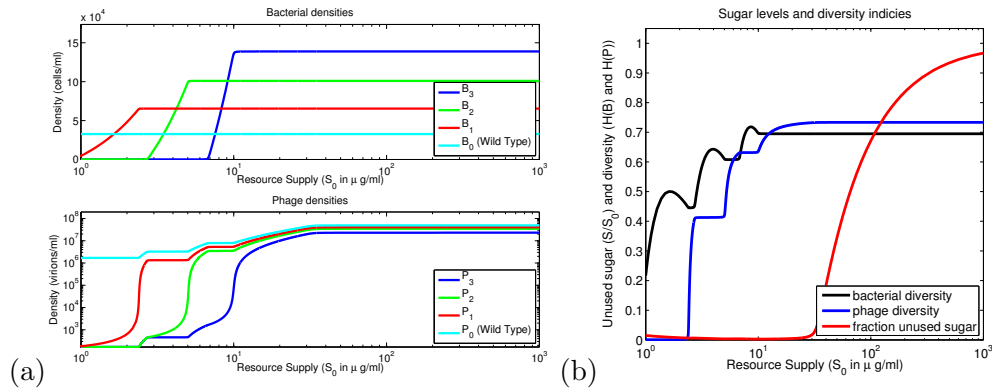


FIGURE 7. Equilibrium densities (see (a)) and diversity (see (b)) of bacteria and phage, also shown is the fraction of unmetabolised resource $(S_0 - S)/S_0$ as a function of resource supply; this uses the same parameters as Figure 5 except that $\Phi = 2 \times 10^{-8} \cdot I_{4 \times 4}$.

The previous example serves to show that one can construct gene-for-gene systems in which the diversity of phage increases with resource supply. The following example illustrates that the gene-for-gene and matching alleles mechanisms cannot therefore be distinguished only on the basis of the diversity patterns they generate.

Example 2. *The space of all gene-for-gene interactions at two genetic loci that also satisfy the uniform adsorption assumption (32) are contained within the following six-parameter family of adsorption matrices:*

$$\Phi_{uaGFG} = \theta \begin{bmatrix} a & b & c & 1 - (a+b+c) \\ 0 & d & 0 & 1 - d \\ 0 & 0 & e & 1 - e \\ 0 & 0 & 0 & 1 \end{bmatrix},$$

where $0 < a, b, c, d, e < 1$ are independent parameters and $\theta > 0$ is a normalisation constant. Proposition 5 applies to the family of matrices defined within Φ_{uaGFG} and we deduce that, modulo an $O(\epsilon)$ correction, phage diversity will increase monotonically with respect to changes in S_0 , when the latter is sufficiently large. This can be seen in the illustrative computation of Figure 8(b) wherein $a = b = c = \frac{1}{4}$ and $d = e = \frac{1}{2}$.

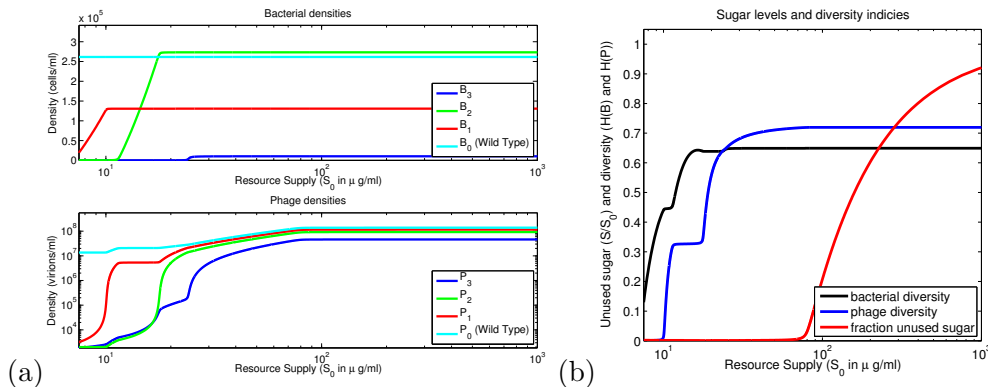


FIGURE 8. Equilibrium densities (see (a)) and diversity (see (b)) of bacteria and phage types, also shown is the fraction of unmetabolised resource $(S_0 - S)/S_0$ as a function of resource supply; this uses the same parameters as Figure 5 except that Φ is given in Example 2 with $\theta = 10^{-8}$.

7. CONCLUSION

We have shown that equation (2) can support at least two distinct long-term diversity patterns: phage diversity can exhibit a *multi-modal* or a *monotonic* dependence on the rate at which energy is supplied to the evolving microcosm, depending on the details of the bacteria-phage infection mechanism.

The model system of *E.coli*-T3 coevolution that we studied empirically lies in the former class. It is not known if the latter class can be realised with an empirical model but the matching allele mechanism has been postulated by others [37] to arise when *E.coli* co-evolves with the coliphage λ . A study of this model system lies beyond the scope of the present article, but this will be the subject of a future study with the aim of providing an appropriate experimental context in which to interpret Figure 7.

ACKNOWLEDGEMENTS

SSA acknowledges support from an ORS award and a studentship from the Department of Mathematics, Imperial College London and IG is supported by NERC EMS and Advanced Fellowships. REB received support from a Medical Research Council Fellowship during this work.

REFERENCES

- [1] A. AGRAWAL AND C. M. LIVELY, *Infection genetics: gene-for-gene versus matching-alleles models and all points in between*, Evolutionary Ecology Research, 4 (2002), pp. 79–90.
- [2] B. J. M. BOHANNAN, B. KERR, C. JESSUP, J. HUGHES, AND G. SANDVIK, *Trade-offs and coexistence in microbial microcosms*, Antonie von Leeuwenhoek, 81 (2002), pp. 107–115.
- [3] B. J. M. BOHANNAN AND R. E. LENSKI, *Linking genetic change to community evolution: insights from studies of bacteria and bacteriophage*, Ecology Letters, 3 (2000), pp. 362–377.
- [4] A. BUCKLING, R. C. MACLEAN, M. A. BROCKHURST, AND N. COLEGRAVE, *The beagle in a bottle*, Nature, 457 (2009), pp. 824–829.
- [5] A. BUCKLING AND P. RAINEY, *Antagonistic coevolution between a bacterium and a bacteriophage*, Proc R Soc Lond, 269 (2002), pp. 931–936.
- [6] J. J. BULL, *Virulence*, Evolution, 48 (1994), pp. 1423–1435.
- [7] J. J. BURDON AND P. H. THRALL, *Spatial and temporal patterns in coevolving plant and pathogen associations*, Am. Nat., 153 (1999), pp. S11–S33.
- [8] L. CHAO, B. LEVIN, AND F. STEWART, *Complex community in a simple habitat - experimental study with bacteria and phage*, Ecology, 58 (1977), pp. 369–378.
- [9] S. CHIBANI-CHENNOUFI, A. BRUTTIN, M. L. DILLMANN, AND H. BRUSSOW, *Phage-host interaction: An ecological perspective.*, J Bact, 186 (2004), pp. 3677–3686.
- [10] W. J. EWANS, *Mathematical Population Genetics I: Theoretical Introduction*, vol. I, Springer Science, 2nd ed., 2004.
- [11] S. E. FORDE, R. E. BEARDMORE, I. GUDELJ, S. S. ARKIN, J. N. THOMPSON, AND L. D. HURST, *Understanding the limits to the generalizability of experimental evolutionary models*, Nature, 455 (2008), pp. 220–223.
- [12] R. I. GAMOW, *Thermodynamic treatment of bacteriophage t4b adsorption kinetics*, Journal of Virology, 4 (1969), pp. 113–115.
- [13] A. HALL AND N. COLEGRAVE, *How does resource supply affect evolutionary diversification?*, Proc. Roy. Soc. B, 274 (2007), pp. 73–78.
- [14] J. IHSSSEN AND T. EGLI, *Specific growth rate and not cell density controls the general stress response in Escherichia coli*, Microbiology, 150 (2004), pp. 1637–1648.
- [15] C. M. JESSUP, R. KASSEN, S. E. FORDE, B. KERR, A. BUCKLING, P. B. RAINEY, AND B. J. M. BOHANNAN, *Big questions, small worlds: microbial model systems in ecology*, TRENDS in Ecology and Evolution, 19 (2004), pp. 189–197.
- [16] T. JUKES AND C. C.R., *Evolution of protein molecules*, vol. Mammalian Protein Metabolism, Academic Press, New York, 1969, pp. 21–132.
- [17] R. KASSEN, A. BUCKLING, G. BELL, AND P. RAINEY, *Diversity peaks at intermediate productivity in a laboratory microcosm*, Nature, 406 (2000), pp. 508–512.
- [18] M. A. LEIBOLD, *Biodiversity and nutrient enrichment in pond plankton communities*, Evolutionary Ecology Research, 1 (1999), pp. 73–95.
- [19] B. R. LEVIN AND J. J. BULL, *Population and evolutionary dynamics of phage therapy*, Nature Reviews Microbiology, (2004), pp. 166–173.

- [20] T. K. LU AND J. J. COLLINS, *Dispersing biofilms with engineered enzymatic bacteriophage*, PNAS, 104 (2007), pp. 11197–11202.
- [21] ———, *Engineered bacteriophage targeting gene networks as adjuvants for antibiotic therapy*, PNAS, (2009). Early Edition, www.pnas.org/cgi/doi/10.1073/pnas.0800442106.
- [22] N. H. MANN, *The third age of phage*, PLoS Biology, 3 (2005), pp. 0753–0755.
- [23] S. K. MAZMANIAN, J. L. ROUND, AND D. L. KASPER, *A microbial symbiosis factor prevents intestinal inflammatory disease*, Nature, 453 (2008), pp. 620–625.
- [24] S. L. MESSENGER, I. J. MOLINEUX, AND J. J. BULL, *Virulence evolution in a virus obeys a trade-off*, Proc. R. Soc. Lond. B Biol. Sci., 266 (1999), pp. 397–404.
- [25] G. G. MITTELBAACH, C. STEINER, S. M. SCHEINER, K. L. GROSS, H. L. REYNOLDS, R. B. WAIDE, M. R. WILLIG, S. I. DODSON, AND L. GOUGH, *What is the observed relationship between species richness and productivity?*, Ecology, 82 (2001), pp. 2381–2396.
- [26] V. POUILLAIN, S. GANDON, M. A. BROCKHURST, A. BUCKLING, AND M. HOCHBERG, *The evolution of specificity in evolving and coevolving antagonistic interactions between a bacteria and its phage*, Evolution, (2007). doi:10.1111/j.1558-5646.2007.00260.x.
- [27] L. M. PRESCOTT, *Microbiology*, McGraw-Hill, 5 ed., 2002.
- [28] U. QIMRON, B. MARINTCHEVA, S. TABOR, AND C. C. RICHARDSON, *Genomewide screens for escherichia coli genes affecting growth of t7 bacteriophage.*, PNAS, 103 (2006), pp. 19039–19044.
- [29] M. SCHWARTZ, *Interaction of Phages with their Receptor Proteins*, vol. Virus Receptors, Part 1 Bacterial Viruses, 1980, pp. 59–94.
- [30] K. SEN AND H. NIKAIDO, *Lipopolysaccharide structure required for invitro trimerization of escherichia-coli ompf porin*, J Bact, 173 (1991), pp. 926–928.
- [31] H. L. SMITH AND P. WALTMAN, *Perturbation of a globally stable steady state*, Proc. AMS, 127 (1999), pp. 447–453.
- [32] W. C. SUMMERS, *Bacteriophage therapy*, Anny. Rev. Microbiol., 55 (2001), pp. 437–451.
- [33] Y. T, N. HAIRSTON, AND S. ELLNER, *Evolutionary trade-off between defence against grazing and competitive ability in a simple unicellular alga, chlorella vulgaris*, Proceeding of the Royal Society of London Series, 271 (2004), pp. 1947–1953.
- [34] L. V. VALEN, *A new evolutionary law*, Evolutionary Theory, 1 (1973), pp. 1–30.
- [35] W. W. TAO, A. MCCANDLISH, L. GRONENBERG, S. CHNG, T. SILHAVY, AND D. KAHNE, *Identification of a protein complex that assembles lipopolysaccharide in the outer membrane of escherichia coli*, PNAS, 103 (2006), pp. 11754–11759.
- [36] R. B. WAIDE, M. R. WILLIG, C. F. STEINER, G. G. MITTELBAACH, L. GOUGH, S. I. DODSON, G. P. JUDAY, AND R. PARMENTER, *The relationship between productivity and species richness*, Annu. Rev. Ecol. Syst., 30 (1999), pp. 235–256.
- [37] J. S. WEITZ, H. HARTMAN, AND L. S. A., *Coevolutionary arms races between bacteria and bacteriophage*, PNAS, 102 (2005), pp. 9535–9540.
- [38] A. ZANGERL AND M. BERENBAUM, *Phenotype matching in wild parsnip and parsnip webworms: Causes and consequences*, Evolution, 57 (2003), pp. 806–815.

R. E. BEARDMORE AND I. GUEDELJ, BIOSCIENCES, STREATHAM CAMPUS, UNIVERSITY OF EXETER, EXETER, UK

S. E. FORDE, DEPARTMENT OF EVOLUTION AND ECOLOGY, UNIVERSITY OF CALIFORNIA, SANTA CRUZ, US